Science

AVAAS

Supplementary Materials for

CRISPR activation and interference screens decode stimulation responses in primary human T cells

Ralf Schmidt *et al.*

Corresponding author: Alexander Marson, alexander.marson@ucsf.edu

The PDF file includes:

Figs. S1 to S20
References

Other Supplementary Material for this manuscript includes the following:

Tables S1 to S6
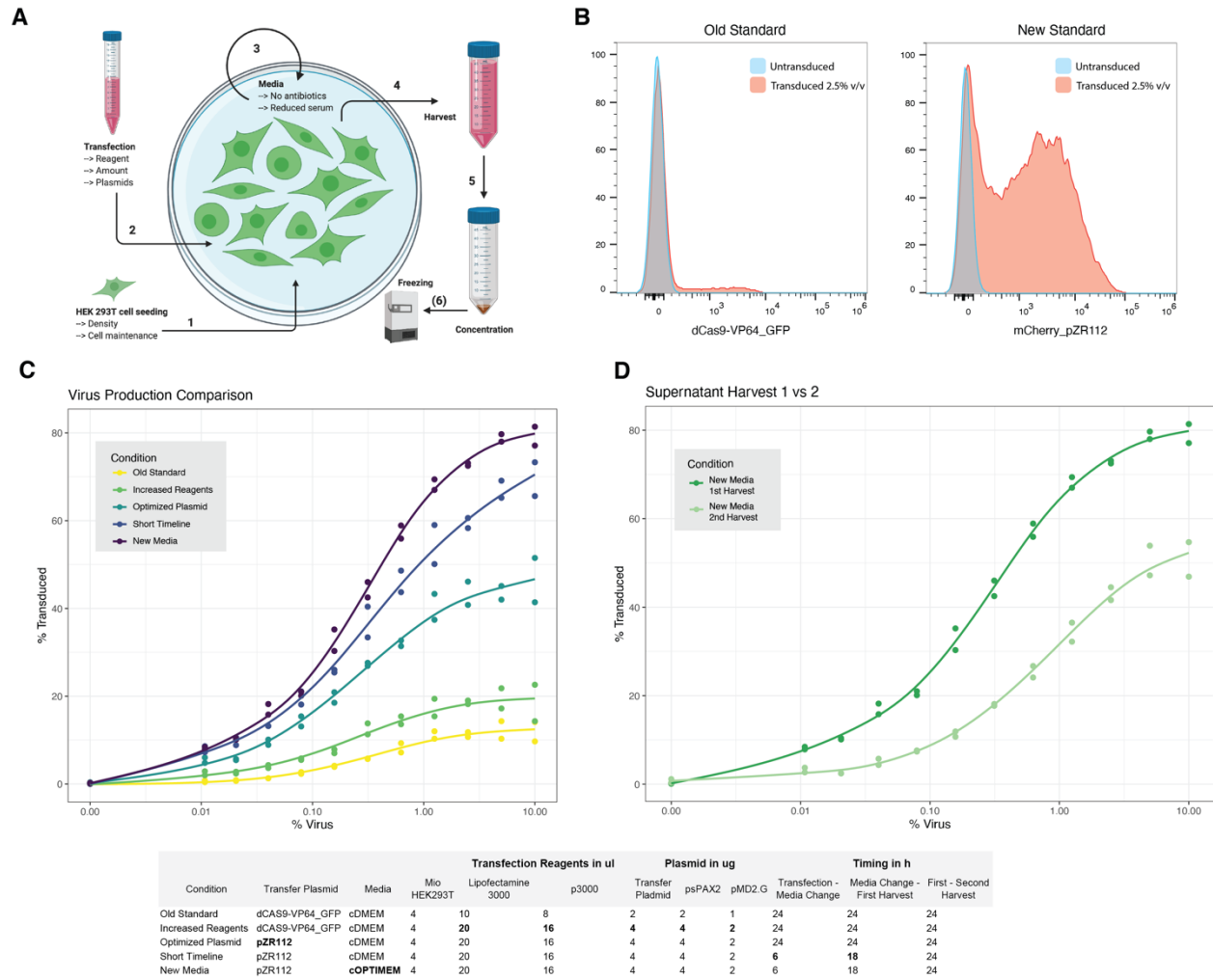MDAR Reproducibility Checklist

Figure S1

Fig. S1. Optimization of lentiviral production and transduction in primary human T cells.
(A) Schematic of factors leading to increased lentiviral titers in production protocols. **(B)** Representative example of transduction using previous vectors and protocols, versus after optimization as measured by flow cytometry. **(C)** Dose-response characterization of transduction efficiencies in primary T cells with indicated factors in lentiviral production. The table below contains full details for each condition. Each point represents percent gated positive for the fluorescent marker. N=2 donors. **(D)** Comparison of transductions after harvesting lentivirus at indicated time points. N=2 donors.
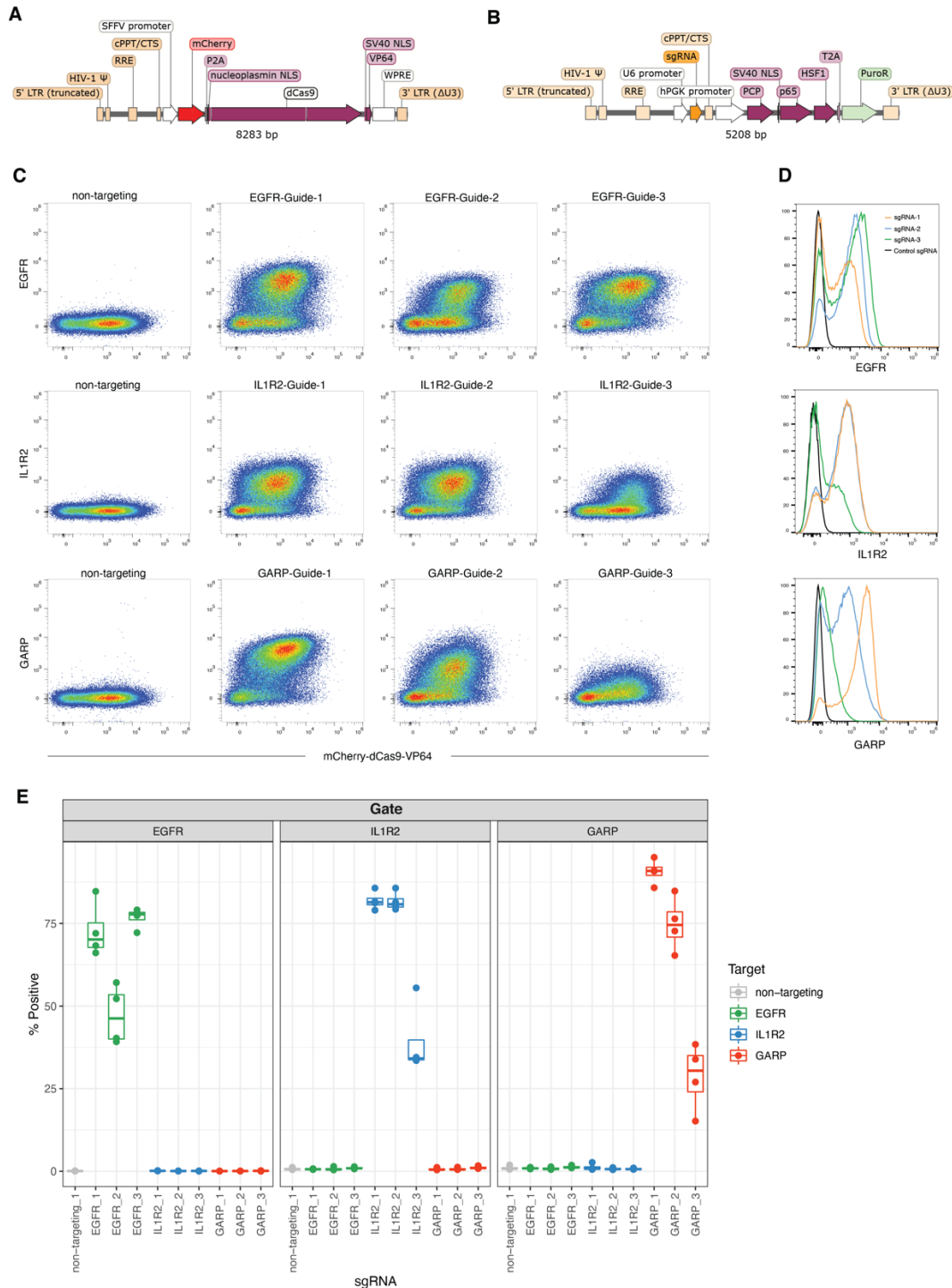
Figure S2

Fig. S2. CRISPRa-SAM system enables robust gene activation in primary human T cells.
(A and B) Lentiviral constructs used for dCas9-VP64 (A) and sgRNA, PCP-P65-HSF1 delivery
(B). **(C and D)** Flow cytometry surface staining after delivery of double dCas9 and sgRNAs
transduction targeting indicated genes or a non-targeting control sgRNA. Scatter plots showing
surface marker correlation with mCherry-2A-dCas9-VP64 expression are shown in (C) and
histograms in (D). **(E)** Quantification of (D) by gating. Points represent percent of cells gated in
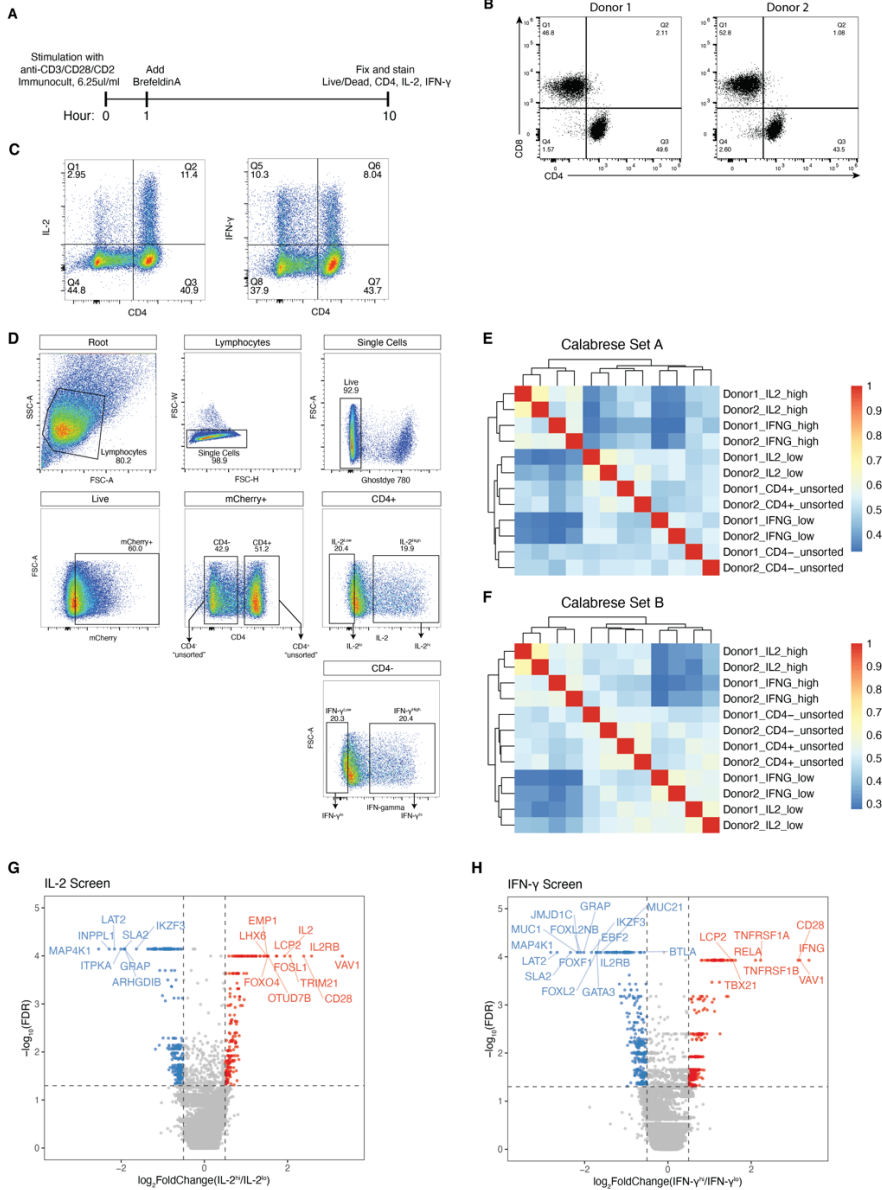each donor. (N=4 donors).

Fig. S3. Genome-wide CRISPRa screens for cytokine production in stimulated primary human T cells. (A) Timeline of restimulation, GolgiPlug with brefeldin A, and fixation/staining. **(B)** Control stain of screen cells with anti-CD8 in addition to anti-CD4. **(C)** Representative flow cytometry plots showing CD4 staining compared to IL-2 and IFN-γ staining. **(D)** Gating strategy used for sorting screens with representative flow cytometry plots. **(E and F)** Pairwise Pearson correlation matrices for Calabrese Set A (E) and Calabrese Set B (F) library samples. Correlations are calculated using sgRNA log2-fold change from the original plasmid pool. **(G and H)** Volcano plots for IL-2 (in CD4+ T cells) (G) and IFN-γ (in CD8+ T cells) (H) screens. Points represent each gene's median log2-fold change followed by averaging two donors with selected gene targets labeled. Dashed lines represent cut-offs for hit calling, with positive and negative hits colored in red and blue, respectively.
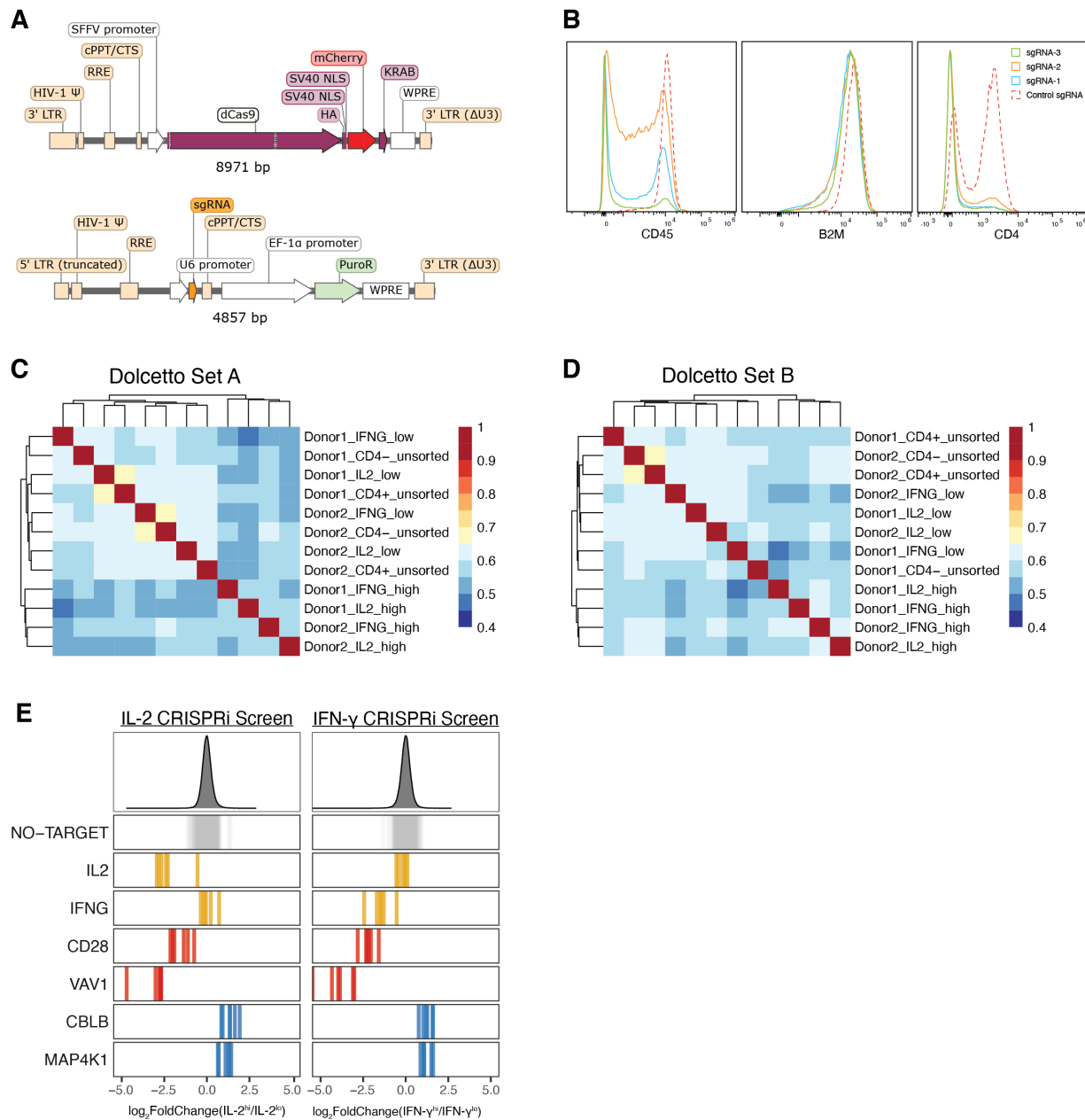
Figure S4

Fig. S4. Genome-wide CRISPRi screens for cytokine production in primary human T cells.
(A) Lentiviral constructs used for dCas9-KRAB and sgRNA delivery. **(B)** Representative
histograms of indicated cell surface protein knockdown after delivery of sgRNAs targeting their
transcriptional start site or a non-targeting control. **(C and D)** Pairwise Pearson correlation
matrices for Dolcetto Set A (C) and Dolcetto Set B (D) library samples. Correlations are
calculated using sgRNA $\log_2$- fold change from the original plasmid pool. **(E)** sgRNA $\log_2$-fold
changes for genes of interest in IL-2 (in CD4$^+$ T cells, left) and IFN-γ (in CD8$^+$ T cells, right)
screens. Bars represent the mean $\log_2$-fold change for each sgRNA across two donors. Density
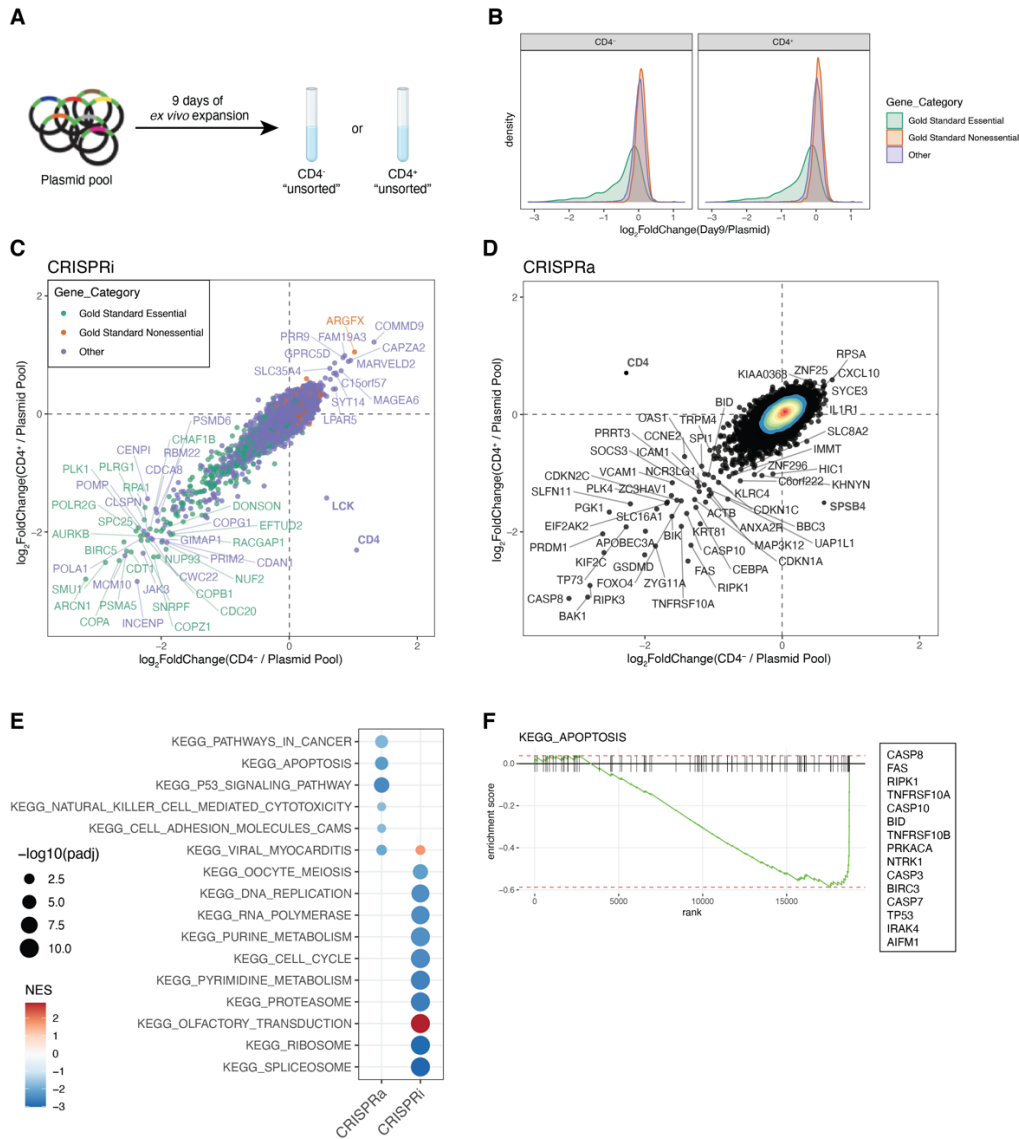plots above represent the distribution of all sgRNAs.

Figure S5

Fig. S5. CRISPRi and CRISPRa dropout screens identify fitness genes. (A) Schematic of samples used for dropout analysis. The sgRNA distribution in the plasmid pool before virus production was compared to the distribution in CD4⁻ and CD4⁺ cells, respectively, without subsorting for cytokines. **(B)** Log_2-fold change distributions of sgRNAs targeting gold-standard essential and nonessential genes in CRISPRi screens. **(C and D)** Gene scatter plot of log_2-fold change from plasmid pool to CD4⁺ and CD4⁻ "unsorted" populations in CRIPSRi (C) and CRISPRa (D) screens. Points represent median of sgRNAs and mean of two donors. Notably, the vast majority of genes are highly correlated, with just *CD4, LCK*, and *SPSB4* discordant (bolded). The *CD4* difference is likely an artifact of the sorting strategy because CD4 knockdown cells will not be found in the CD4⁺ gate. Perturbations affecting *LCK*, and *SPSB4* may also cause loss of CD4 expression. **(E)** GSEA of KEGG pathways significantly enriched in CRISPRa and CRISPRi dropout screens. Points are scaled to $-log_{10}$ FDR adjusted *P*-value. **(F)** GSEA of KEGG Apoptosis pathway in CRISPRa dropout. Top ranked genes in the set are listed on the right.
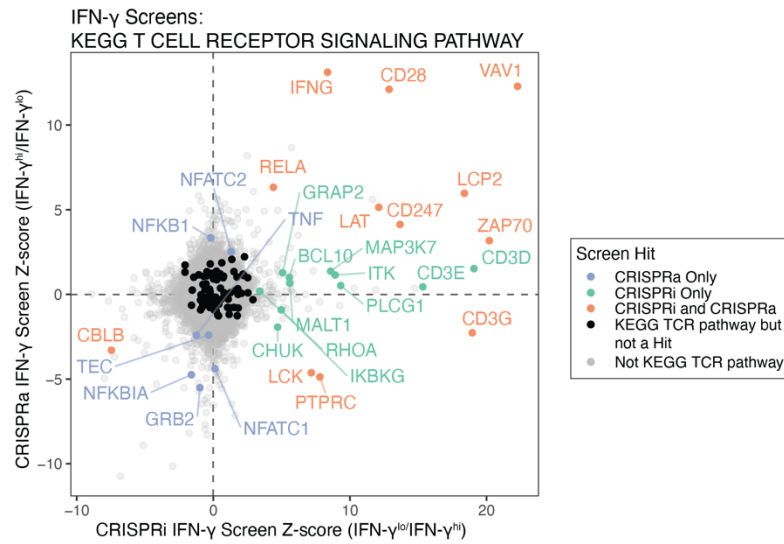
Figure S6

Fig. S6. Comparison IFN-γ CRISPRi and CRISPRa screens for genes belonging to the T cell receptor signaling pathway. Genes annotated as T cell receptor signaling pathway (KEGG pathways) are indicated in colors other than gray. Scales represent Z-score of $\log_2$-fold change, with positive regulators of IFN-γ production having positive Z-scores.
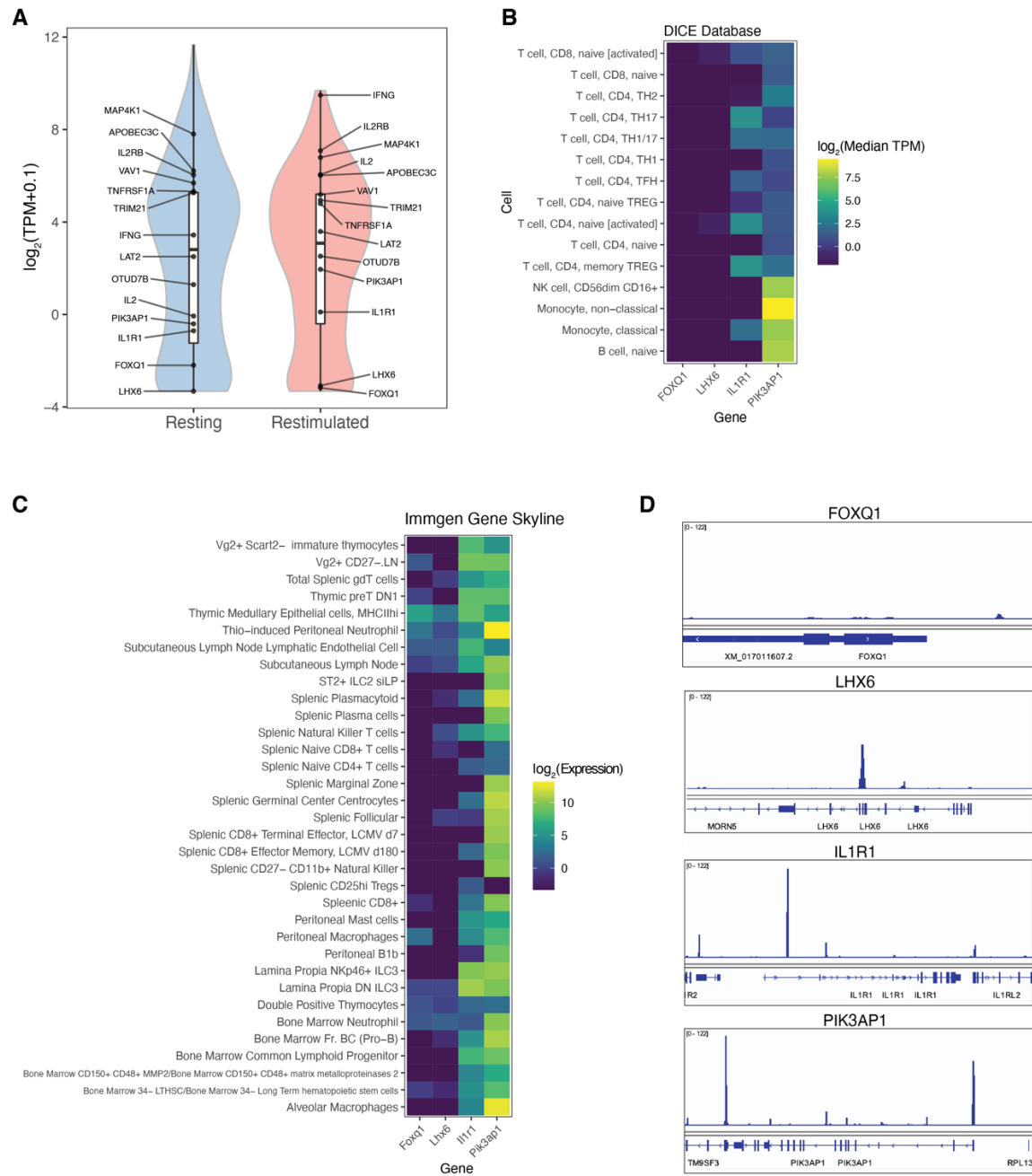
Figure S7

Fig. S7. Expression of CRISPRa hits of interest in immune cells. (A) Distributions of gene mRNA expression of CRISPRa cytokine screen hits in resting and restimulated CD4$^+$ T cells in control CRISPRa cells transduced with non-targeting sgRNAs (see methods, "Bulk RNA-seq"). The expression of genes tested in the arrayed sgRNA panel (Fig. 3B) are indicated. **(B)** Heatmap showing the expression of indicated genes in indicated human immune cell types, from the Database of Immune Cell Expression (DICE) (*57*). Values represent the median log$_2$TPM for each gene. **(C)** Heatmap showing the expression of indicated genes in indicated mouse immune cells, from the Immunological Genome Project (Immgen) gene skyline database (*58*). **(D)** ATAC-seq tracks from unstimulated human CD3$^+$ T cells (from ENCODE ID ENCSR258RSH) for indicated genes.
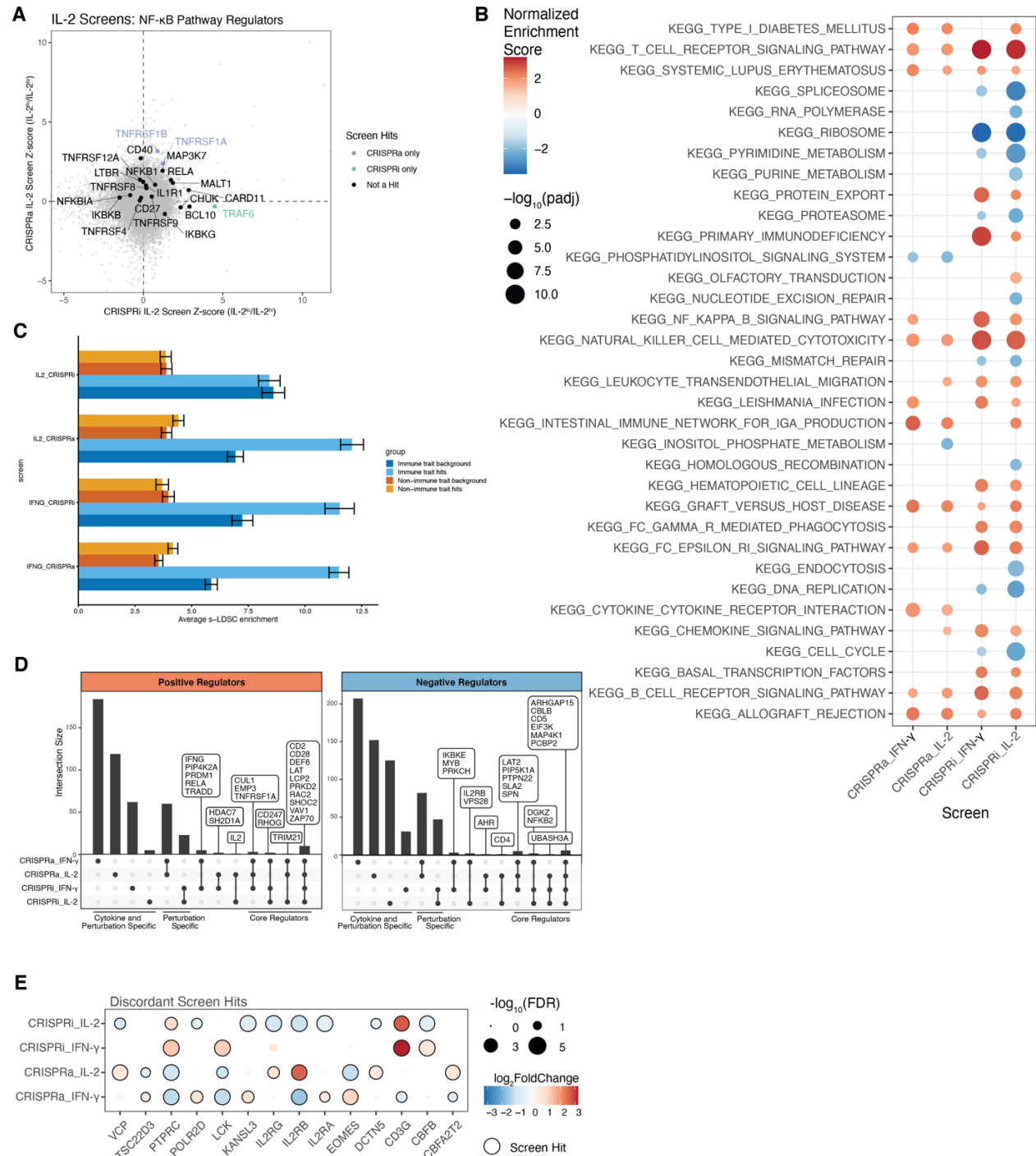
Figure S8

Fig. S8. Pathway gene set enrichment in CRISPRa and CRISPRi cytokine screens.
(A) Comparison IL-2 CRISPRi and CRISPRa screens with NF-κB pathway regulators of interest labeled. **(B)** Significantly enriched KEGG pathways from CRISPRa/CRISPRi screen log$_2$-fold change gene ranks. Points are scaled according to $-\log_{10}$ FDR adjusted *P*-value. **(C)** s-LDSC enrichment of heritability for immune and non-immune traits in a window of 100 kb around genes that were hits in the indicated screens. Traits were meta-analyzed using inverse-

variance weighting; bars represent average enrichment ± standard error. **(D)** Unique and common positive and negative regulators identified across CRISPRa and CRISPRi screens. For CRISPRa, positive regulators are defined as having a positive $\log_2$-fold change (high/low bins), and for CRISPRi a negative $\log_2$-fold change (high/low). **(E)** Discordant hits across CRISPRi and CRISPRa hits for IL-2 in CD4$^+$ T cell and IFN-γ in CD8$^+$ T cell screens, where perturbations identified as positive regulators are colored and red, and negative regulators in blue. Discordant hits between IL-2 and IFN-γ screens include *EOMES* and *CBFB*, encoding transcription factors known to have key roles in the differentiation of T cell subsets. The proximal kinase responsible for CD3ζ phosphorylation, LCK, and its activating phosphatase, CD45 (encoded by *PTPRC*), are discordant between CRISPRi and CRISPRa screens, suggesting appropriately balanced expression in this module is critical for optimal TCR signal transduction.
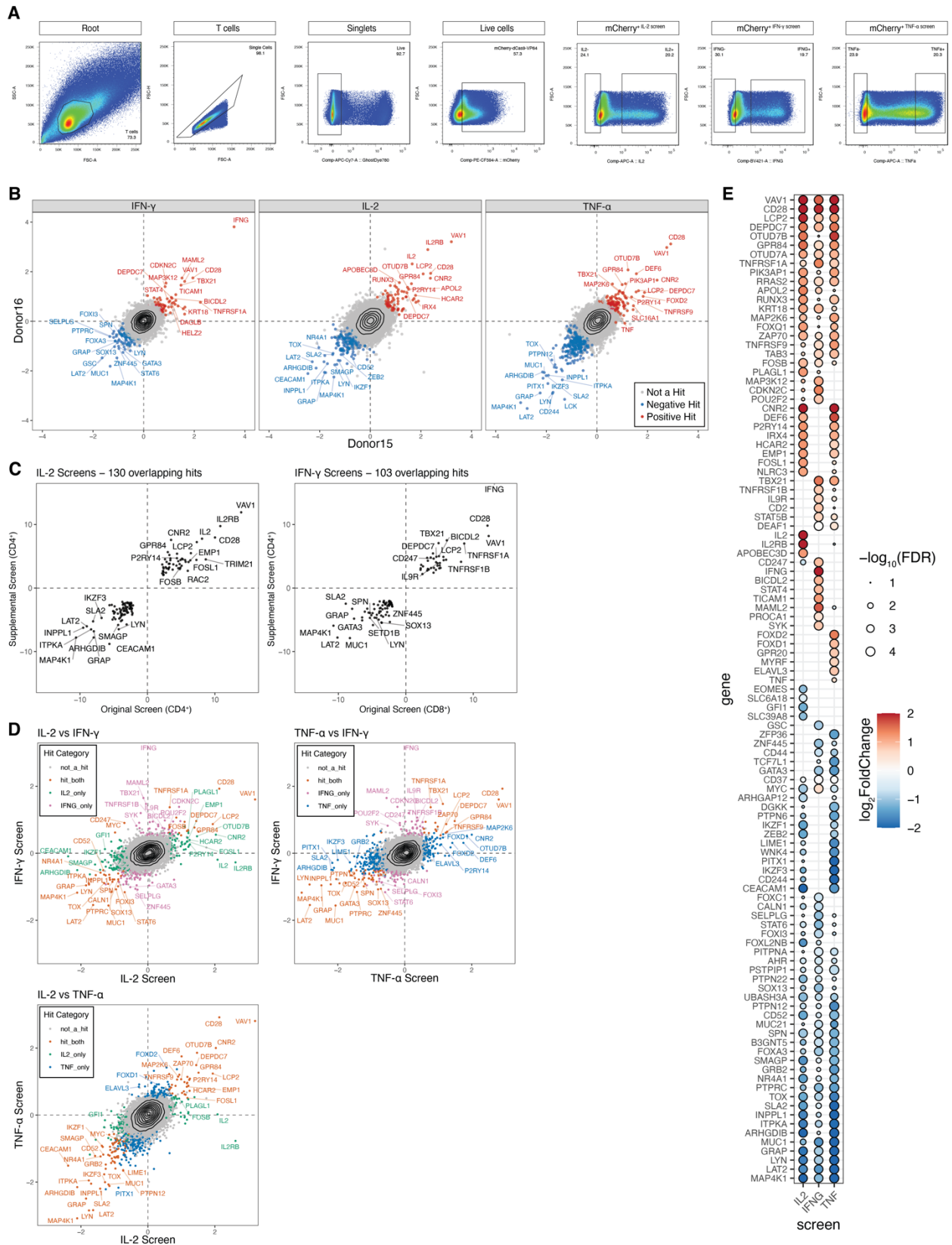
Figure S9

Fig. S9. Genome-wide CRISPRa screens for cytokine production in CD4+ T cells allow for direct comparison of cytokine regulators. (A) Gating strategy for screens. Isolated CD4+ T

cells were sorted according to the strategy shown here. **(B)** Scatter plots of median sgRNA $\log_2$-fold change (high/low sorting bins) for each gene, comparing screens in two blood donors, for indicated cytokine screens. **(C)** Scatter plots comparing common hits in primary CRISPRa screens in CD4$^+$/CD8$^+$ T cells (Fig. 1), and CD4$^+$ only screens. Commons hits are defined as FDR<0.05 and an absolute $\log_2$-fold change Z-score >2 in both screens. **(D)** Scatter plot comparisons of gene median $\log_2$-fold change values in these three supplemental screens for different cytokines in CD4$^+$ T cells. **(E)** Heatmap comparison of top positive and negative hits in these supplemental CD4$^+$ T cell screens. Genes with a top-25 ranking by MAGeCK are shown. Only points with an FDR<0.1 are shown.
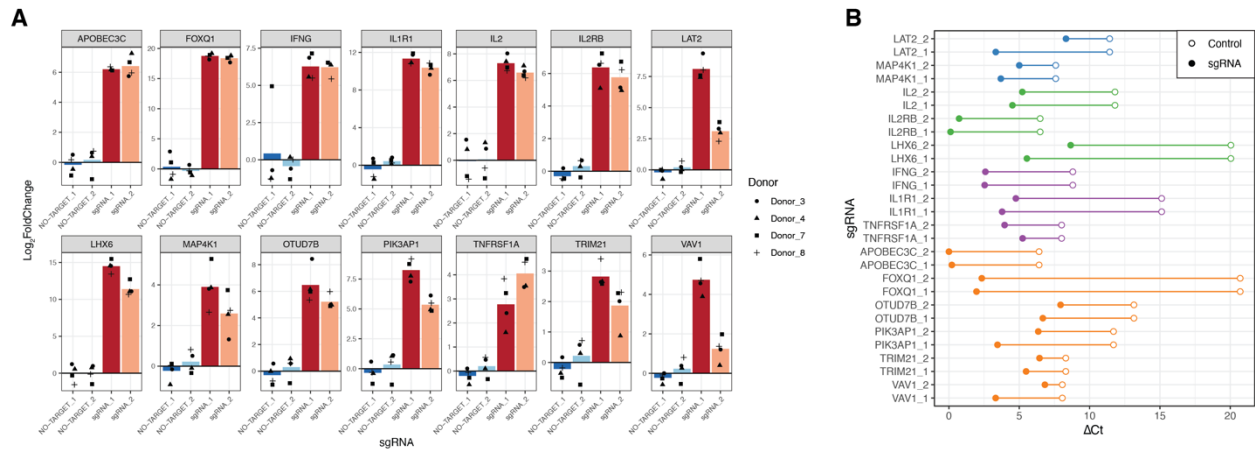
Figure S10

Fig. S10. RT-qPCR validation of on-target gene activation in an arrayed CRISPRa panel.
(A) Log$_2$-fold change in mRNA expression for target sgRNAs compared to mean of non-targeting controls. Each facet represents the measurement of the indicated transcript and its measurement with two non-targeting control sgRNAs or two sgRNAs targeting its TSS. **(B)** deltaCt summary of (A), showing mean non-targeting controls and mean targeting sgRNA deltaCt values for each sgRNA. N=4 human donors.
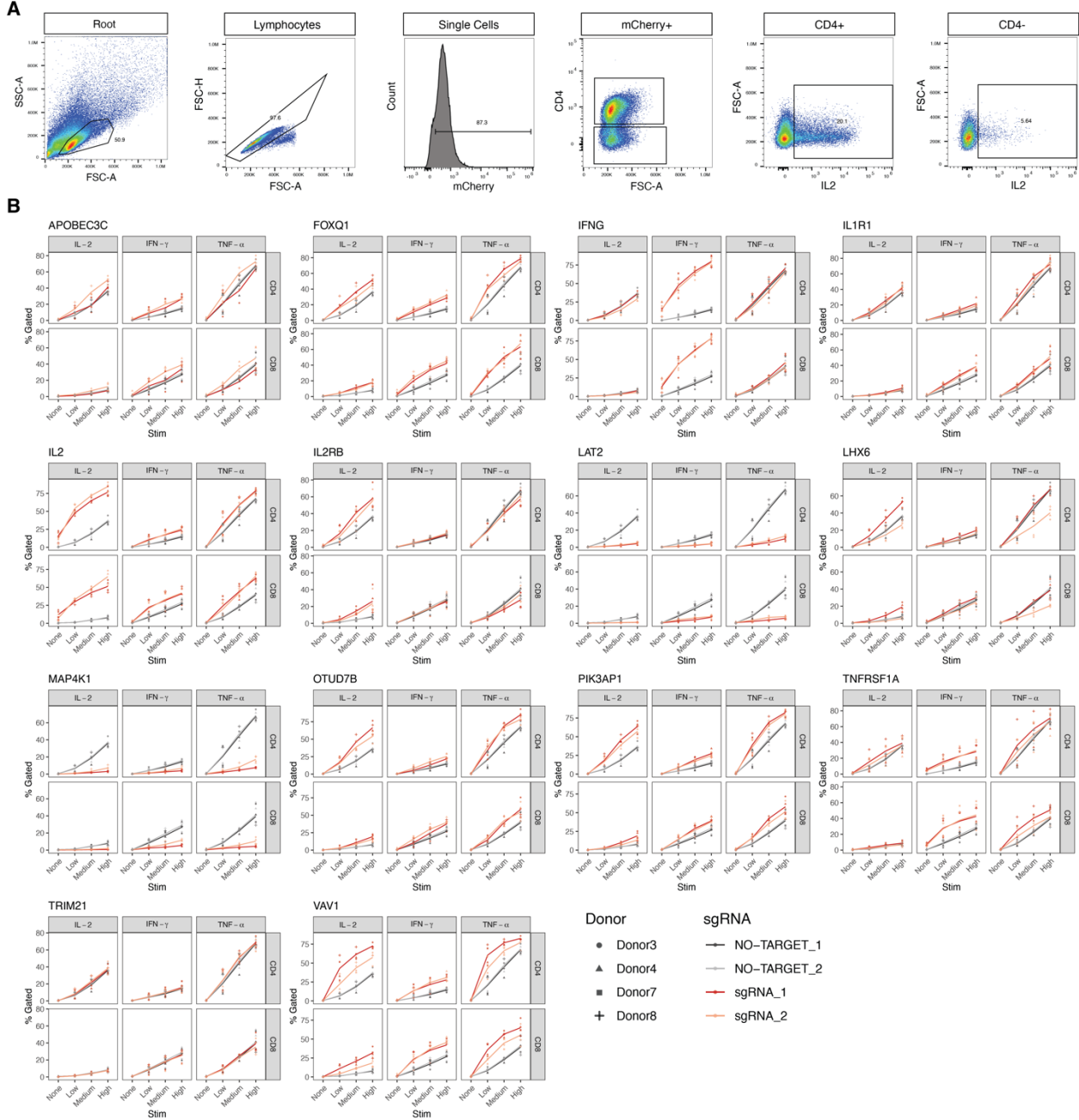
Figure S11

Fig. S11. Flow cytometry staining in an arrayed CRISPRa panel. (A) Schematic of gating strategy. Note, IFN-γ and TNF-α are not shown here, but follow the same strategy as IL-2. **(B)** Complete data of summary shown in Fig. 3D. Points represent the percentage of cells gated as positive for expressing a given cytokine in the indicated donors, across multiple stimulation doses. Low, medium, and high doses represent 3.125, 6.25, and 12.5 μl/ml of anti-CD3/CD28/CD2 ImmunoCult, respectively.
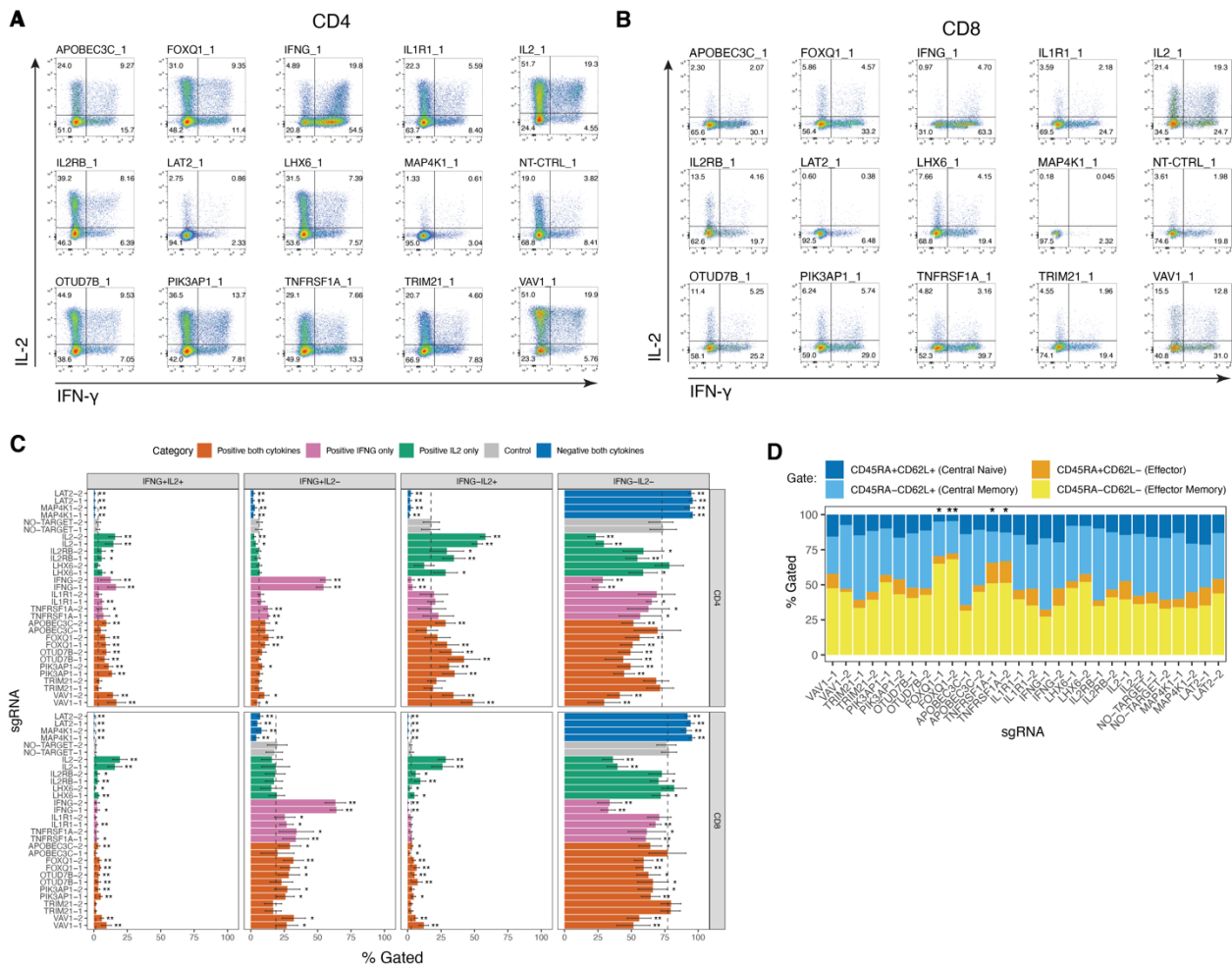
Figure S12

Fig. S12. Examining the single-cell relationship between IL-2 and IFN-γ production in arrayed CRISPRa panel by flow cytometry. Given that IL-2 and IFN-γ can be expressed from mutually exclusive populations (*59*), we asked if CRISPRa-driven changes in IL-2 and IFN-γ cytokine production are driven by single or double-positive cells. We observed that most positive regulator sgRNAs could increase both the single and double-positive populations. **(A and B)** Representative flow cytometry plots of intracellular IFN-γ and IL-2 staining with indicated sgRNAs in CD4+ (A) or CD8+ (B) T cells. Two-dimensional gates for double-negative, single-positive, and double-positive populations are shown. **(C)** Quantifications of IFN-γ/IL-2 two-dimensional gating. Bars represent mean ± standard deviation. *q<0.05, **q<0.01. Mann–Whitney *U* test with q-value multiple comparison correction. N=4 donors. (D) Surface staining gating for CD45RA and CD62L of resting CD4+ T cells transduced with the arrayed sgRNA panel. *P<0.05, **P<0.01 Mann–Whitney *U* test, testing for percent CD62L+.
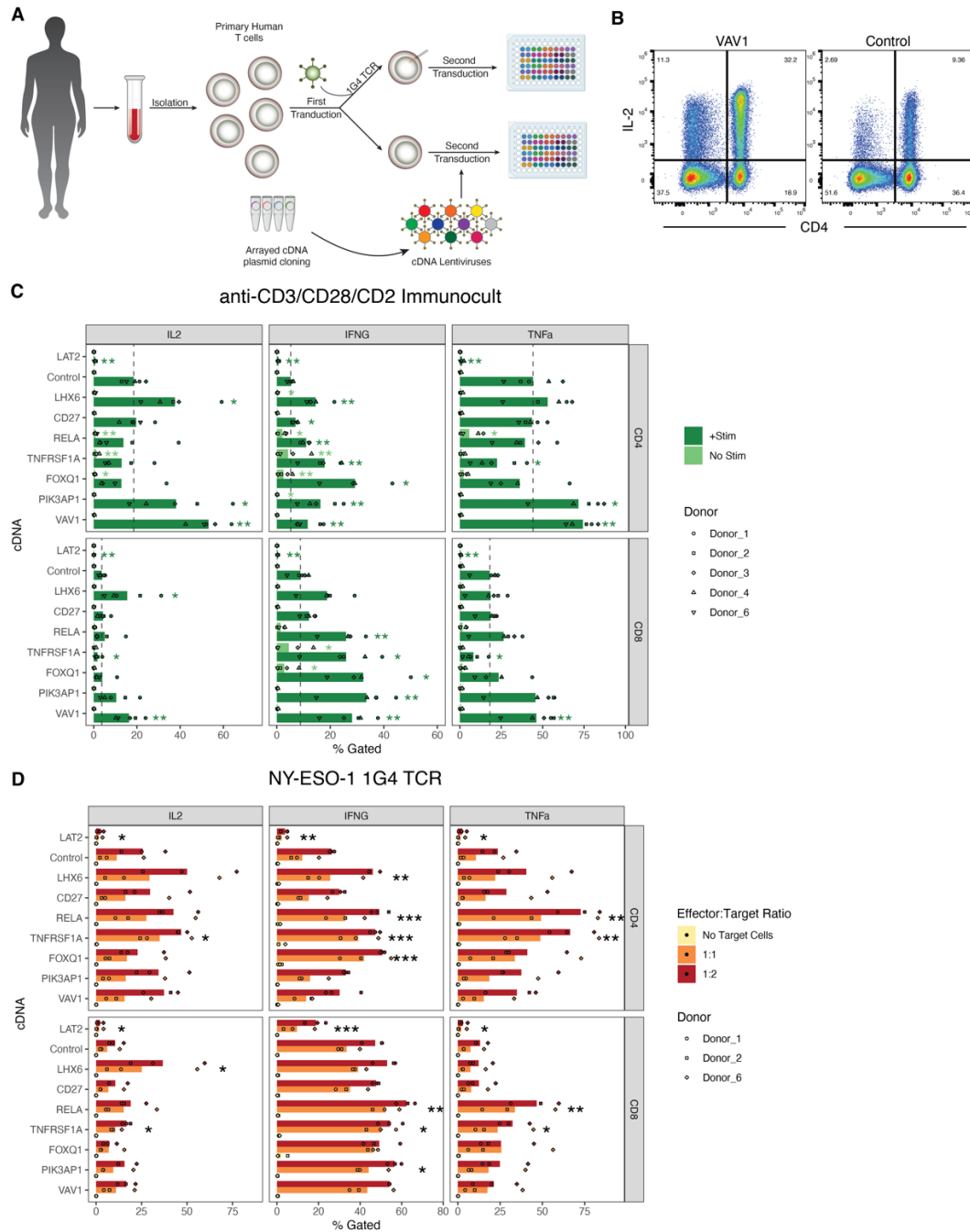
Figure S13

Fig. S13. CRISPRa gain-of-function findings can translate to transgenic cDNA overexpression and TCR stimulation with antigen. (A) Schematic of arrayed overexpression experiments with cDNA**. (B)** Flow cytometry plot for *VAV1* or Control cDNA (puromycin resistance only) overexpression after stimulation with Immunocult. **(C)** Mean Percentage of cells in cytokine positive gates from after stimulation with Immunocult. *$P<0.05$, **$P<0.01$, Mann–Whitney U test compared to control. N=5 Donors. **(D)** Mean Percentage of cells in cytokine positive gates after stimulation with NALM6 target cells engineered to express NY-ESO-1 antigen in an HLA-A0201 context at multiple effector-to-target cell ratios. *$P<0.05$, **$P<0.01$, ***$P<0.001$, two-way dose-response ANOVA compared to control. N=3 Donors (Two donors were excluded due to poor TCR transduction).
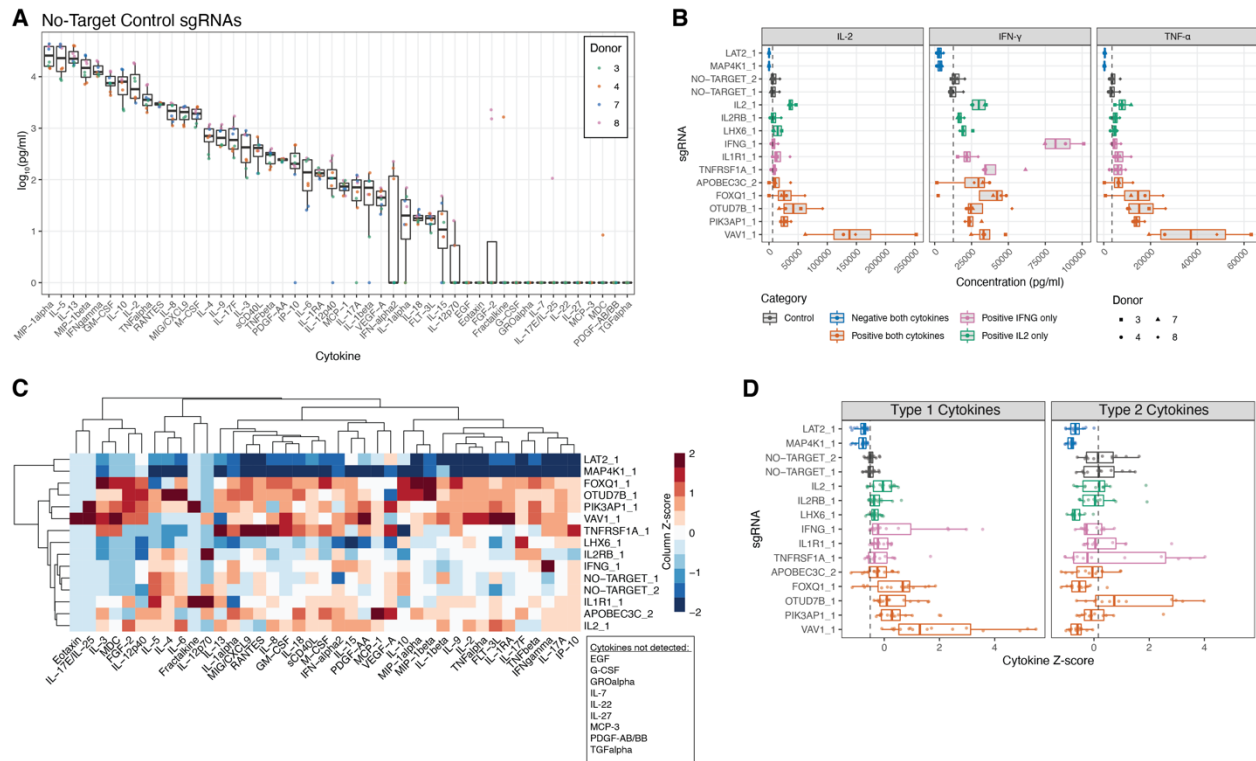
Figure S14

Fig. S14. Secreted cytokine measurements in an arrayed CRISPRa panel. (A) Cytokine measurements of 4 human donors in two non-targeting control sgRNA samples after stimulation (2 individual sgRNAs). **(B)** Measurements of IL-2, IFN-γ, and TNF-α in samples with indicated sgRNAs. N=4 Donors. The effect of *IL2RB* on IL-2 production was not concordant with intracellular staining, perhaps due to reuptake caused by increased IL-2 receptor levels. **(C)** Unsupervised clustering of full cytokine panel measurements across different sgRNAs. Each tile represents the median value of 4 donors, Z-score scaled across each cytokine. **(D)** Type 1 and Type 2 category grouped cytokine measurements across different sgRNAs. N=4 Donors. Type 1 group includes IFN-γ, IL-2, TNF-α, and TNF-β. Type 2 group includes IL-4, IL-5, and IL-13. Each point represents a donor, cytokine measurement, Z-score scaled for each cytokine.
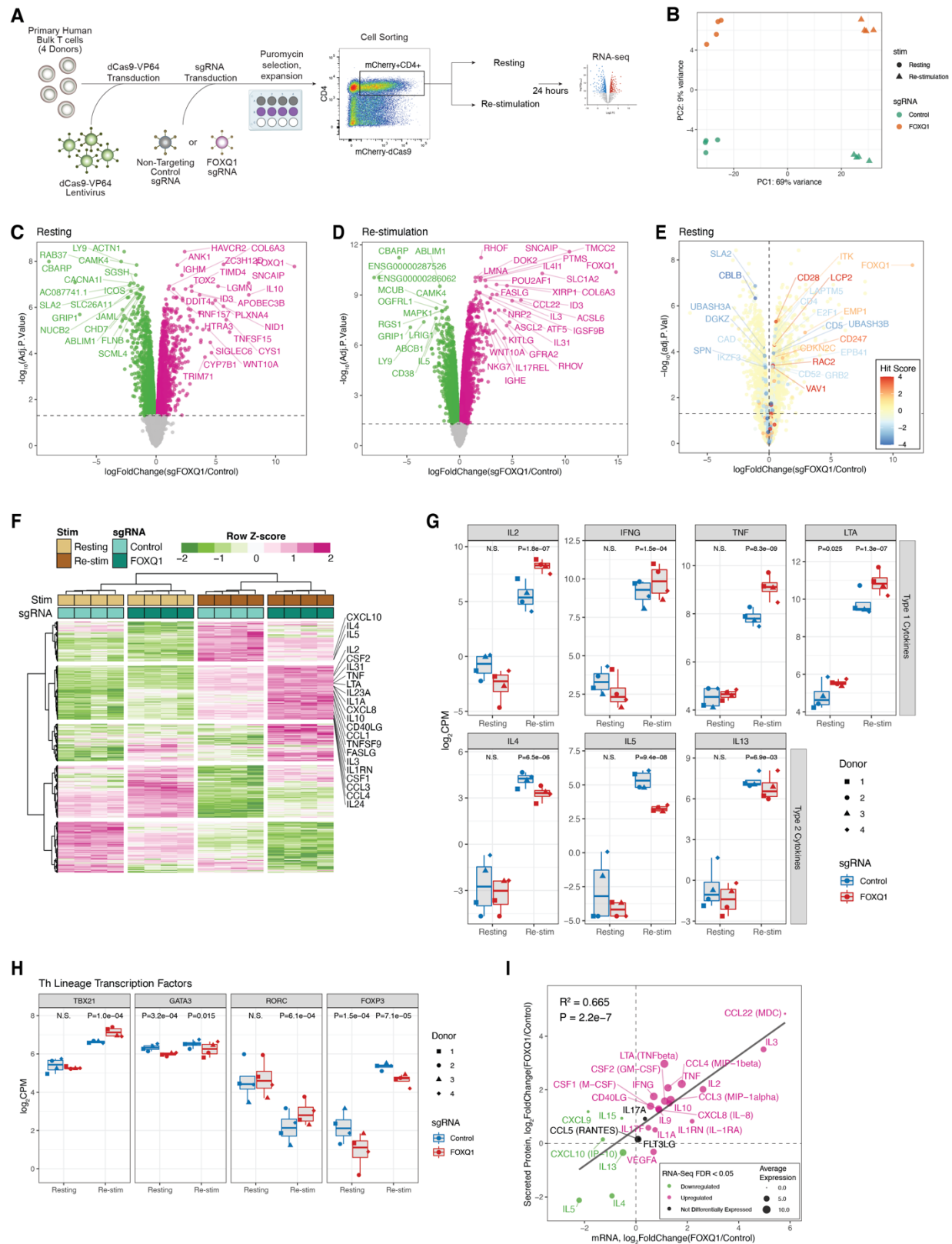
Figure S15

Fig. S15. *FOXQ1* overexpression transcriptionally reshapes the cytokine response in CD4$^+$ T cells. (A) Schematic of RNA-seq experiment in CD4$^+$ T cells after *FOXQ1* overexpression via CRISPRa. **(B)** PCA across all samples in RNA-seq transcript quantifications. **(C and D)** Differential gene expression volcano plots, between *FOXQ1* sgRNA and non-targeting control sgRNA in resting (C) and stimulated (D) T cells. **(E)** Differential expression volcano plot of *FOXQ1* sgRNA versus non-targeting control in non-stimulated cells colored according to hit score, where hit score is defined as the number of screens which identified the gene was identified as a positive regulator (positive hit score) or negative regulator (negative hit score) of cytokine production. *FOXQ1* overexpression increased expression of core cytokine regulators identified in the CRISPRa and CRISPRi screens (*CD28, LCP2, RAC2, VAV1*) and reduced expression of core negative regulators (*CBLB, SLA2*), suggesting FOXQ1 may sensitize T cells to stimulation by increasing overall levels of proximal signaling components. **(F)** Heatmap representation of *FOXQ1* differentially expressed genes across all samples shows that *FOXQ1* overexpression remodels the T cell stimulation response. Selected genes represent any that have an FDR adjusted *P*-value $<10^{-4}$ in *FOXQ1* sgRNA versus control differential expression tests. Selected cytokine genes of interest are indicated on the right. **(G)** mRNA expression of Type 1 signature cytokine genes (*IL2, IFNG, TNF, LTA*), and Type 2 signature cytokine genes (*IL4, IL5, IL13*) across RNA-seq samples shows that *FOXQ1* overexpression amplifies Type 1 signature cytokines and dampens Type 2 signature cytokines compared to control. FDR adjusted *P*-values between control and *FOXQ1* sgRNA samples are shown at top. **(H)** mRNA expression of T helper cell lineage defining transcription factors across RNA-seq samples. FDR adjusted *P*-values between control and *FOXQ1* sgRNA samples are shown at top. *TBX21* defines Th1, *GATA3* defines Th2, *RORC* defines Th17, and *FOXP3* defines Treg. **(I)** Comparison of $\log_2$-fold changes in mRNA and secreted protein expression (Fig. 3H and fig. S14) resulting from *FOXQ1* overexpression. *FOXQ1* overexpression drove transcriptional modulation of cytokine genes, which correlated well with secreted cytokine measurements.
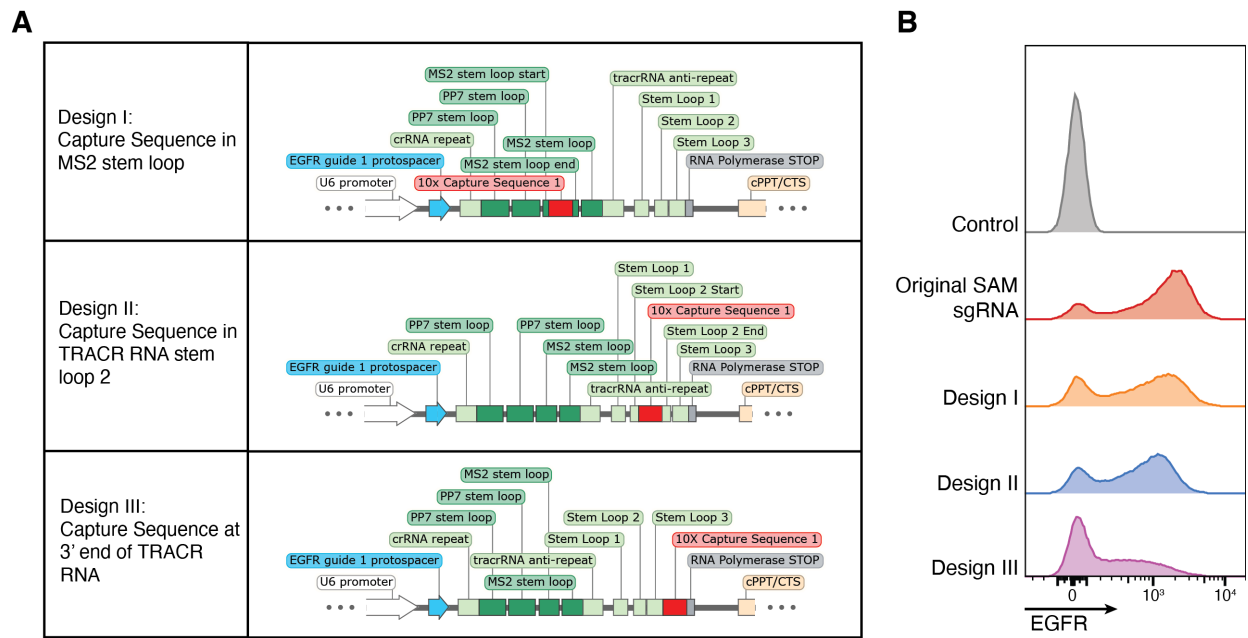
Figure S16

Fig. S16. Development of sgRNA direct-capture CRISPRa-SAM Perturb-seq. (A) Overview of candidate sgRNA vector designs with direct-capture sequence integrated at various points of the SAM modified sgRNA scaffold. **(B)** Flow cytometry to measure gene activation with test sgRNA targeting *EGFR* using constructs described in (A). Design I was chosen for the CRISPRa Perturb-seq experiment because of its gene activation efficacy and its predicted fragment size compatibility with 10x Genomics library preparation protocols.
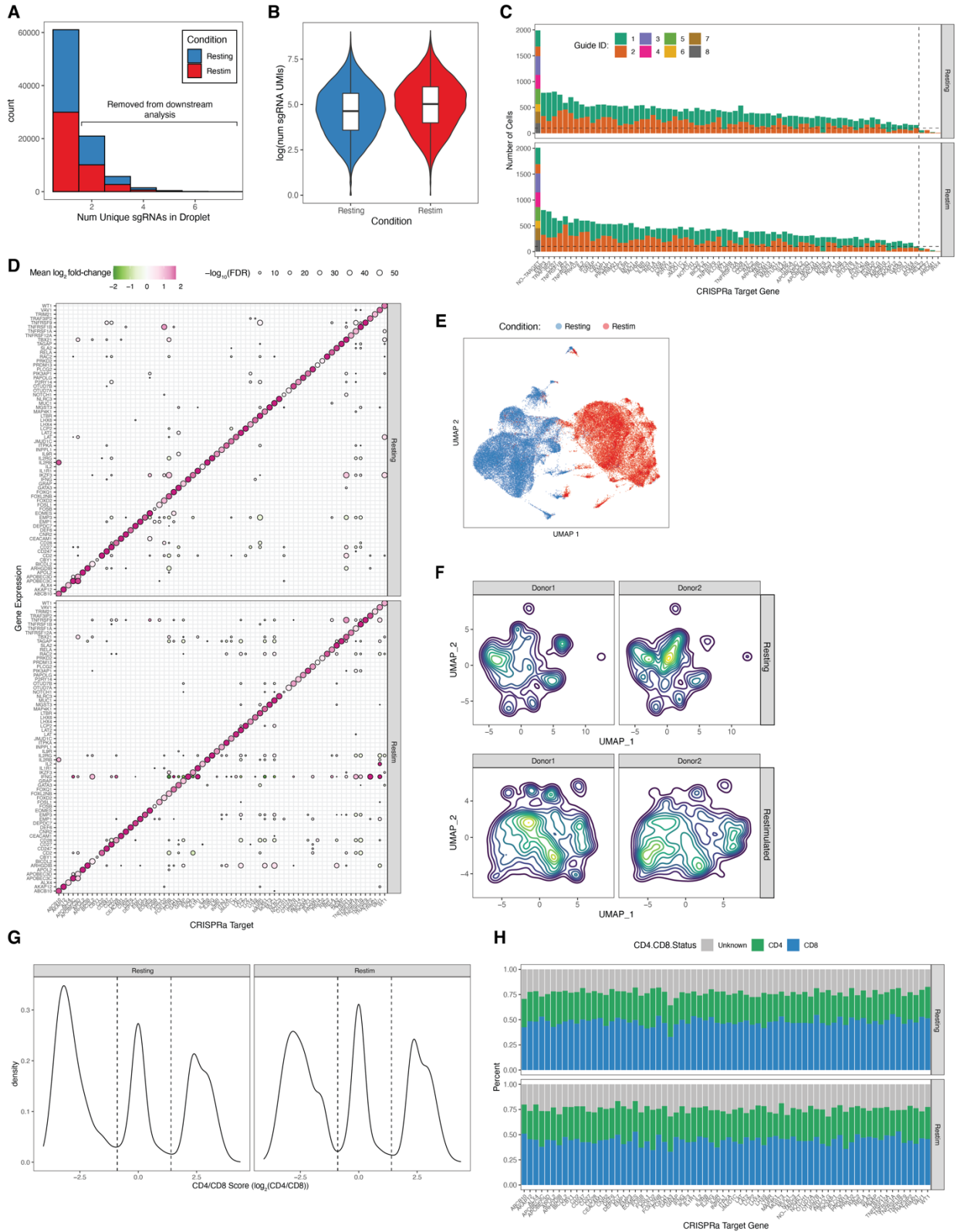
Figure S17

Fig. S17. Direct-capture CRISPRa Perturb-seq assigns sgRNAs to cells. (A) Histogram of number of sgRNAs detected per droplet. Droplets with >1 sgRNA were removed from downstream analysis **(B)** Distribution of the number of sgRNA unique molecular indices (UMIs) detected in each singlet shown in (A). **(C)** Number of cells assigned to each sgRNA in the library. sgRNAs targeting genes with <100 assigned cells (right of dashed lines) in the restimulated or resting conditions were removed from downstream analysis. **(D)** Heatmap of differential expression of CRISPRa target genes in the Perturb-seq library. Points represent differential expression of cells assigned to sgRNAs (*x*-axis) over no-target control cells for the indicated genes' expression (*y*-axis). **(E)** UMAP projection of all cells colored by resting or restimulated conditions. **(F)** Contour density plots of cells assigned to indicated donors in UMAP space. **(G)** Distribution of CD4/CD8 scores in both conditions. Dashed lines represent the cutoffs for calling cells as CD4$^+$ or CD8$^+$. **(H)** Fraction of CD4$^+$, CD8$^+$, or undefined cells for cells assigned to each sgRNA target. The majority of undefined cells was due to no detection of either *CD4* or *CD8A/CD8B* transcripts.
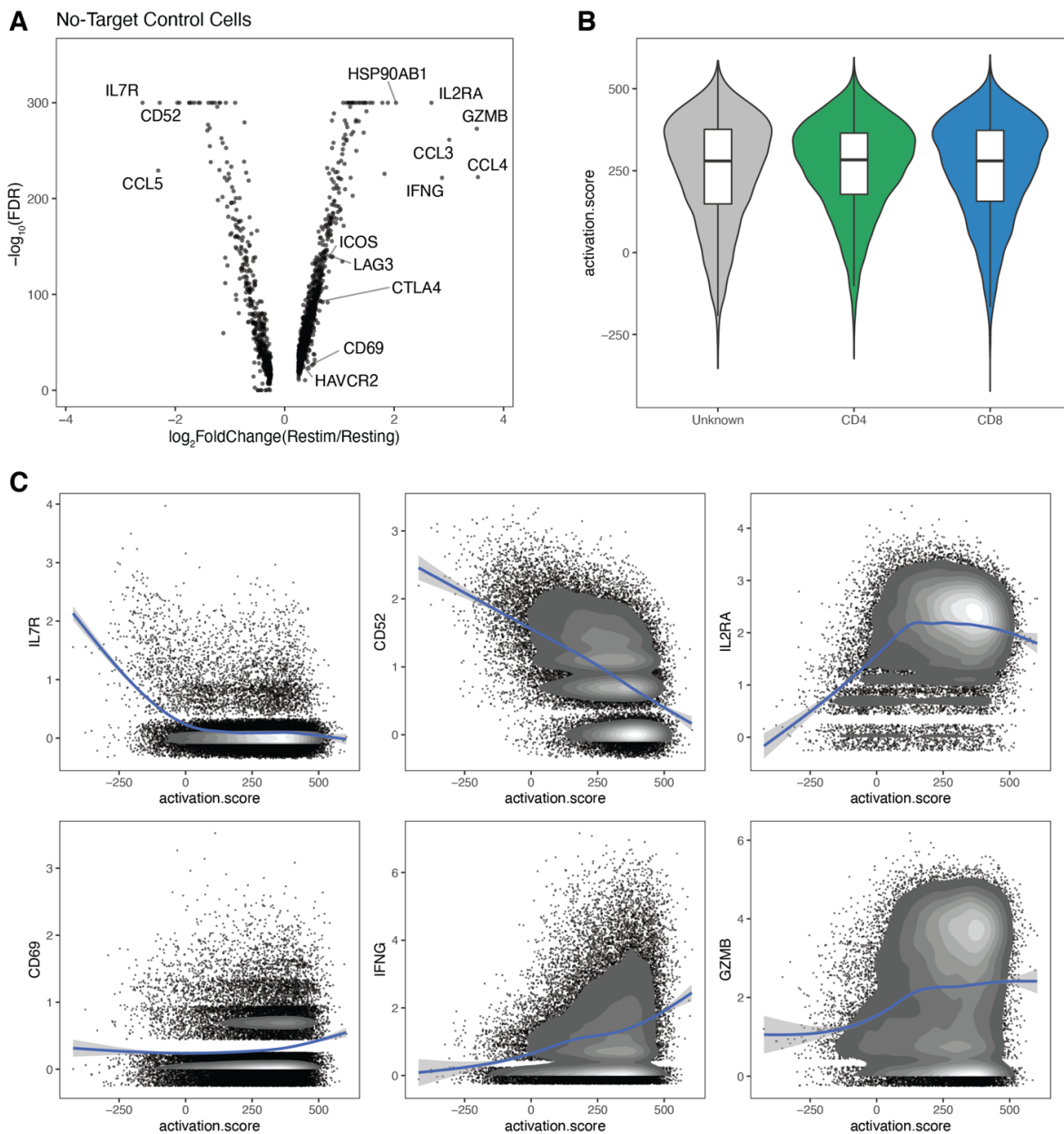
Figure S18

Fig. S18. Developing a T cell activation gene signature score. (A) Volcano plot showing differential expression of genes in no-target sgRNA control cells between resting and restimulated conditions. Top differentially expressed genes and manually selected commonly used activation markers are indicated. Only genes with an absolute $\log_2$-fold change >0.25, and detected in 10% of restimulated or resting cells are shown. Activation scores are weighted by $\log_2$-fold change values shown here. **(B)** Violin plots showing the distributions of activation scores CD4^{+}, CD8^{+}, and undefined T cells in the restimulated condition. **(C)** Scatter plots of all cells in the restimulated condition, comparing activation scores with expression of single negative markers of activation (*IL7R, CD52*) and positive markers of activation (*IL2RA, CD69, IFNG, GZMB*). Generalized additive models are shown in blue.
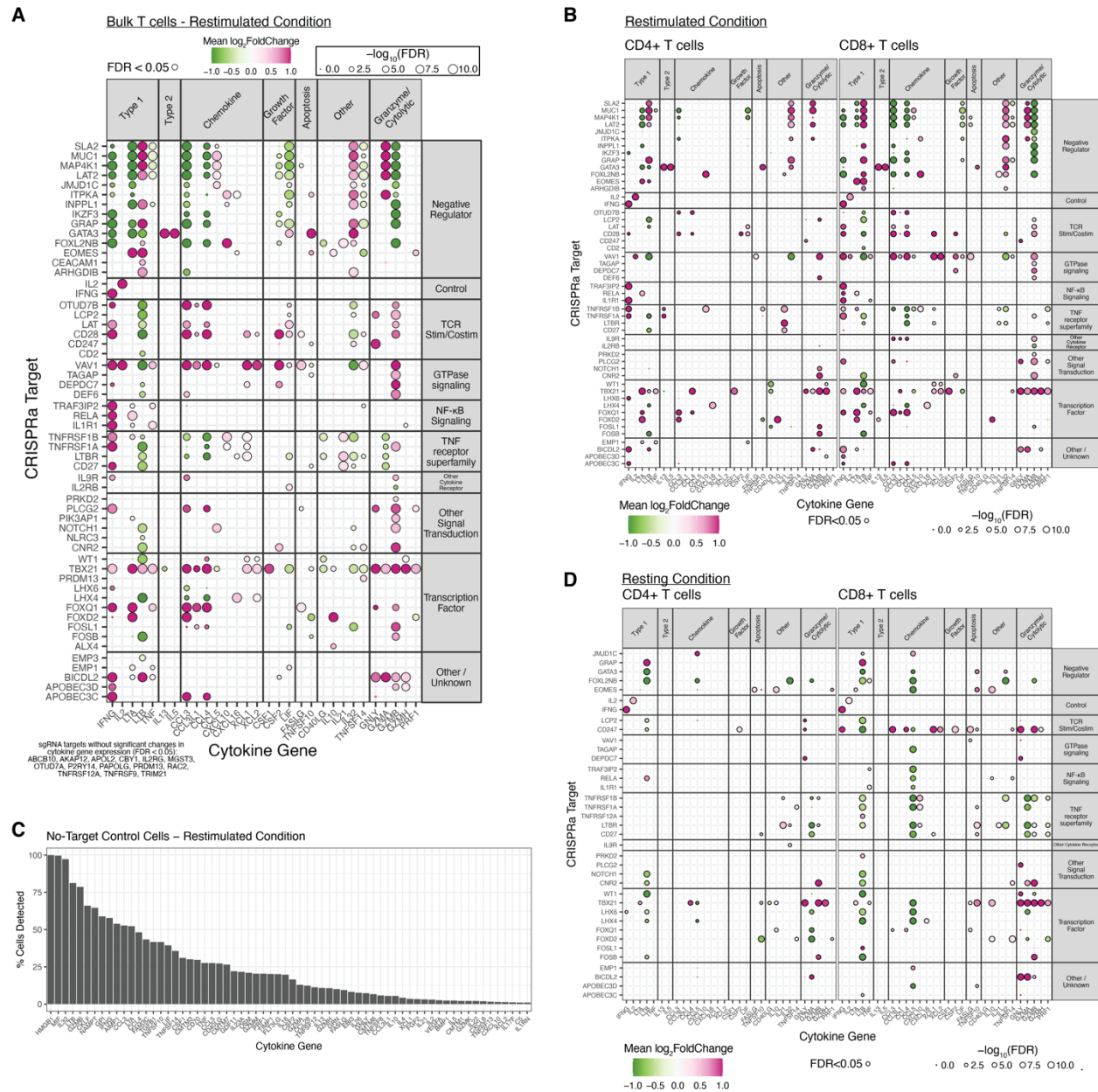
Figure S19

Fig. S19. Differential expression of cytokine/effector genes by CRISPRa Perturb-seq. (A and B) Pseudobulk differential expression analysis of cytokine/effector genes for cells assigned to indicated sgRNAs, compared to no-target control cells for all T cells (A) or split by CD4+/CD8+ assignment (B) in the restimulated conditions. Only cytokine/effector genes with substantial detection in the dataset were analyzed (detected in >20% of cells in at least 1 sgRNA group). Only sgRNA targets with >=1 statistically significant (FDR<0.05) differentially expressed cytokine gene are shown. **(C)** Percent of no-target control cells in the restimulated condition with the indicated cytokine/effector gene transcript detected. Cytokine genes (GO:0005125) with <1% of cells having a detected transcript are not shown. **(D)** Pseudobulk differential expression of cytokine genes in resting condition in the same format as (B).
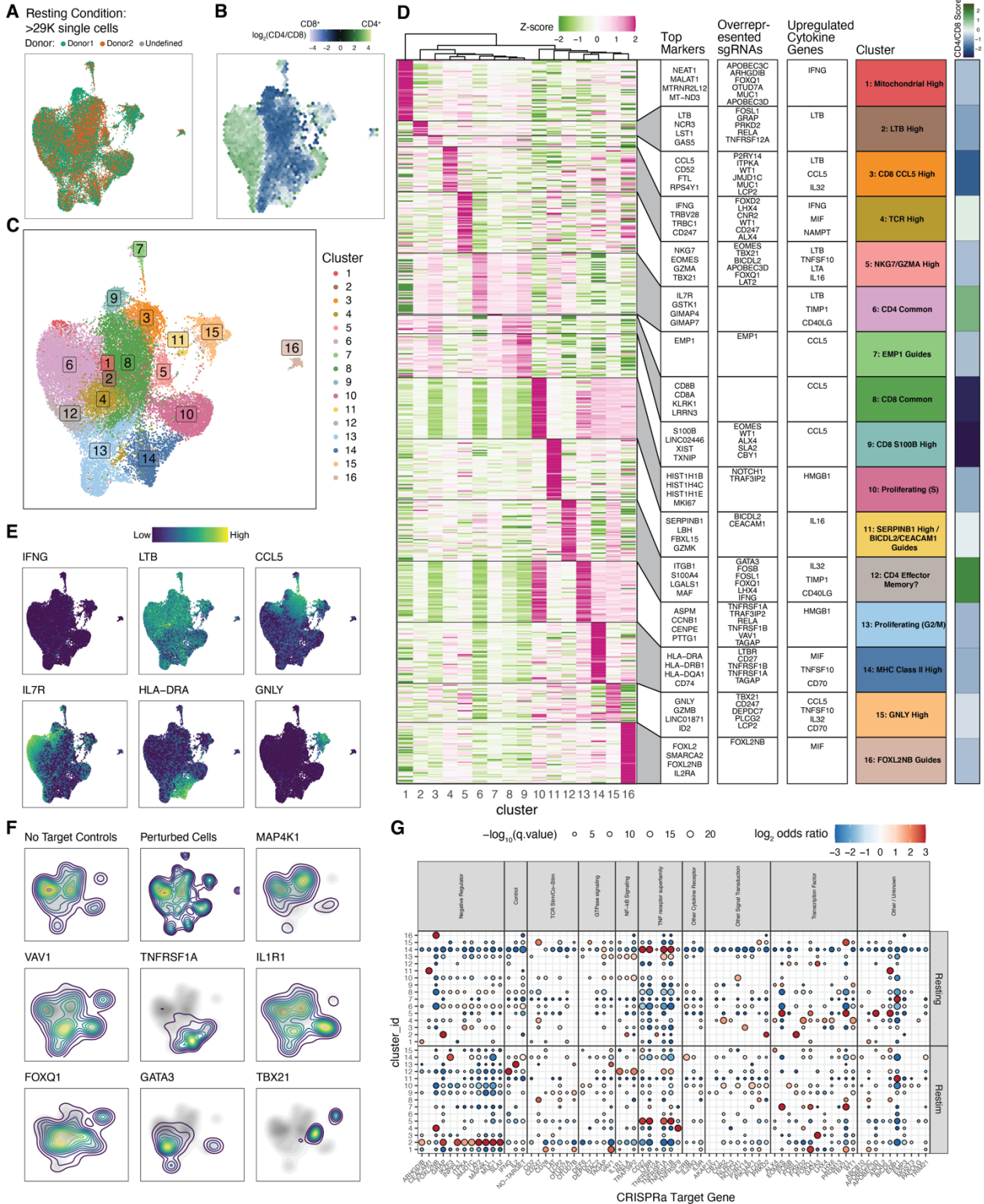
Figure S20

Fig. S20. Unsupervised clustering of CRISPRa Perturb-seq T cells in resting condition. (A) UMAP projection of post-quality control filtered resting T cells, colored by donor. **(B)** Distribution of CD4⁺ and CD8⁺ T cells across resting T cell UMAP projection. Each bin is colored by the average log_2(CD4/CD8) transcript levels of cells in that bin. **(C)** Resting T cell UMAP with cells colored by cluster. **(D)** Heatmap of differentially expressed marker genes in

each cluster. The top 50 statistically significant (FDR<0.05) differentially upregulated genes for each cluster are shown, with genes that are upregulated in multiple clusters being given priority to the cluster with the higher $\log_2$ fold change for the given gene. The top marker genes by $\log_2$-fold change in each clusters' section are listed to the right. Top overrepresented sgRNAs in each cluster by odds ratio are listed to the next right (full data represented in G). Top differentially upregulated cytokine genes in each cluster are listed to the next right. Mean cell $\log_2$(CD4/CD8) cell transcript values in each cluster are shown on the far right. **(E)** Resting T cell UMAP with the expression of indicated genes shown. **(F)** Contour density plots of resting cells assigned to indicated sgRNA targets in UMAP space. The no-target control contour is shown in greyscale underneath. "Perturbed Cells" represents all cells that did not receive a no-target control sgRNA. **(G)** Heatmap of sgRNA target over/under-representation in clusters shown in Fig. 4G and fig. S20C. Fisher's exact test with q-value multiple comparison correction. Only interactions with a q<0.05 are shown.

References and Notes

1. A. K. Abbas, E. Trotta, D. R Simeonov, A. Marson, J. A. Bluestone, Revisiting IL-2: Biology and therapeutic prospects. *Sci. Immunol.* **3**, eaat1482 (2018). doi:10.1126/sciimmunol.aat1482 Medline

2. L. Ni, J. Lu, Interferon gamma in cancer immunotherapy. *Cancer Med.* **7**, 4509–4516 (2018). doi:10.1002/cam4.1700 Medline

3. F. Castro, A. P. Cardoso, R. M. Gonçalves, K. Serre, M. J. Oliveira, Interferon-gamma at the crossroads of tumor immune surveillance or evasion. *Front. Immunol.* **9**, 847 (2018). doi:10.3389/fimmu.2018.00847 Medline

4. L. B. Ivashkiv, IFNγ: Signalling, epigenetics and roles in immunity, metabolism, disease and cancer immunotherapy. *Nat. Rev. Immunol.* **18**, 545–558 (2018). doi:10.1038/s41577-018-0029-z Medline

5. T. R. Malek, The biology of interleukin-2. *Annu. Rev. Immunol.* **26**, 453–479 (2008). doi:10.1146/annurev.immunol.26.021607.090357 Medline

6. D. A. Boardman, M. K. Levings, Cancer immunotherapies repurposed for use in autoimmunity. *Nat. Biomed. Eng.* **3**, 259–263 (2019). doi:10.1038/s41551-019-0359-6 Medline

7. J. Gao, L. Z. Shi, H. Zhao, J. Chen, L. Xiong, Q. He, T. Chen, J. Roszik, C. Bernatchez, S. E. Woodman, P.-L. Chen, P. Hwu, J. P. Allison, A. Futreal, J. A. Wargo, P. Sharma, Loss of IFN-γ pathway genes in tumor cells as a mechanism of resistance to anti-CTLA-4 therapy. *Cell* **167**, 397–404.e9 (2016). doi:10.1016/j.cell.2016.08.069 Medline

8. J. M. Zaretsky, A. Garcia-Diaz, D. S. Shin, H. Escuin-Ordinas, W. Hugo, S. Hu-Lieskovan, D. Y. Torrejon, G. Abril-Rodriguez, S. Sandoval, L. Barthly, J. Saco, B. Homet Moreno, R. Mezzadra, B. Chmielowski, K. Ruchalski, I. P. Shintaku, P. J. Sanchez, C. Puig-Saus, G. Cherry, E. Seja, X. Kong, J. Pang, B. Berent-Maoz, B. Comin-Anduix, T. G. Graeber, P. C. Tumeh, T. N. M. Schumacher, R. S. Lo, A. Ribas, Mutations associated with acquired resistance to PD-1 blockade in melanoma. *N. Engl. J. Med.* **375**, 819–829 (2016). doi:10.1056/NEJMoa1604958 Medline

9. M. Ayers, J. Lunceford, M. Nebozhyn, E. Murphy, A. Loboda, D. R. Kaufman, A. Albright, J. D. Cheng, S. P. Kang, V. Shankaran, S. A. Piha-Paul, J. Yearley, T. Y. Seiwert, A. Ribas, T. K. McClanahan, IFN-γ-related mRNA profile predicts clinical response to PD-1 blockade. *J. Clin. Invest.* **127**, 2930–2940 (2017). doi:10.1172/JCI91190 Medline

10. R. R. Bartelt, N. Cruz-Orcutt, M. Collins, J. C. D. Houtman, Comparison of T cell receptor-induced proximal signaling and downstream functions in immortalized and primary T cells. *PLOS ONE* **4**, e5430 (2009). doi:10.1371/journal.pone.0005430 Medline

11. H. Colin-York, S. Kumari, L. Barbieri, L. Cords, M. Fritzsche, Distinct actin cytoskeleton behaviour in primary and immortalised T-cells. *J. Cell Sci.* **133**, jcs.232322 (2019). doi:10.1242/jcs.232322 Medline

12. E. Astoul, C. Edmunds, D. A. Cantrell, S. G. Ward, PI 3-K and T-cell activation: Limitations of T-leukemic cell lines as signaling models. *Trends Immunol.* **22**, 490–496 (2001). doi:10.1016/S1471-4906(01)01973-1 Medline

13. O. Parnas, M. Jovanovic, T. M. Eisenhaure, R. H. Herbst, A. Dixit, C. J. Ye, D. Przybylski, R. J. Platt, I. Tirosh, N. E. Sanjana, O. Shalem, R. Satija, R. Raychowdhury, P. Mertins, S. A. Carr, F. Zhang, N. Hacohen, A. Regev, A genome-wide CRISPR screen in primary immune cells to dissect regulatory networks. *Cell* **162**, 675–686 (2015). doi:10.1016/j.cell.2015.06.059 Medline

14. M. B. Dong, G. Wang, R. D. Chow, L. Ye, L. Zhu, X. Dai, J. J. Park, H. R. Kim, Y. Errami, C. D. Guzman, X. Zhou, K. Y. Chen, P. A. Renauer, Y. Du, J. Shen, S. Z. Lam, J. J. Zhou, D. R. Lannin, R. S. Herbst, S. Chen, Systematic immunotherapy target discovery using genome-scale in vivo CRISPR screens in CD8 T cells. *Cell* **178**, 1189–1204.e23 (2019). doi:10.1016/j.cell.2019.07.044 Medline

15. J. Henriksson, X. Chen, T. Gomes, U. Ullah, K. B. Meyer, R. Miragaia, G. Duddy, J. Pramanik, K. Yusa, R. Lahesmaa, S. A. Teichmann, Genome-wide CRISPR screens in T helper cells reveal pervasive crosstalk between activation and differentiation. *Cell* **176**, 882–896.e18 (2019). doi:10.1016/j.cell.2018.11.044 Medline

16. E. Shifrut, J. Carnevale, V. Tobin, T. L. Roth, J. M. Woo, C. T. Bui, P. J. Li, M. E. Diolaiti, A. Ashworth, A. Marson, Genome-wide CRISPR screens in primary human T cells reveal key regulators of immune function. *Cell* **175**, 1958–1971.e15 (2018). doi:10.1016/j.cell.2018.10.024 Medline

17. P. Y. Ting, A. E. Parker, J. S. Lee, C. Trussell, O. Sharif, F. Luna, G. Federe, S. W. Barnes, J. R. Walker, J. Vance, M.-Y. Gao, H. E. Klock, S. Clarkson, C. Russ, L. J. Miraglia, M. P. Cooke, A. E. Boitano, P. McNamara, J. Lamb, C. Schmedt, J. L. Snead, Guide Swap enables genome-scale pooled CRISPR-Cas9 screening in human primary cells. *Nat. Methods* **15**, 941–946 (2018). doi:10.1038/s41592-018-0149-1 Medline

18. D. R. Simeonov, B. G. Gowen, M. Boontanrart, T. L. Roth, J. D. Gagnon, M. R. Mumbach, A. T. Satpathy, Y. Lee, N. L. Bray, A. Y. Chan, D. S. Lituiev, M. L. Nguyen, R. E. Gate, M. Subramaniam, Z. Li, J. M. Woo, T. Mitros, G. J. Ray, G. L. Curie, N. Naddaf, J. S. Chu, H. Ma, E. Boyer, F. Van Gool, H. Huang, R. Liu, V. R. Tobin, K. Schumann, M. J. Daly, K. K. Farh, K. M. Ansel, C. J. Ye, W. J. Greenleaf, M. S. Anderson, J. A. Bluestone, H. Y. Chang, J. E. Corn, A. Marson, Discovery of stimulation-responsive immune enhancers with CRISPR activation. *Nature* **549**, 111–115 (2017). doi:10.1038/nature23875 Medline

19. Y. Liu, C. Yu, T. P. Daley, F. Wang, W. S. Cao, S. Bhate, X. Lin, C. Still 2nd, H. Liu, D. Zhao, H. Wang, X. S. Xie, S. Ding, W. H. Wong, M. Wernig, L. S. Qi, CRISPR activation screens systematically identify factors that drive neuronal fate and reprogramming. *Cell Stem Cell* **23**, 758–771.e8 (2018). doi:10.1016/j.stem.2018.09.003 Medline

20. X. Chen, L. Kozhaya, C. Tastan, L. Placek, M. Dogan, M. Horne, R. Abblett, E. Karhan, M. Vaeth, S. Feske, D. Unutmaz, Functional interrogation of primary human T cells via CRISPR genetic editing. *J. Immunol.* **201**, 1586–1598 (2018). doi:10.4049/jimmunol.1701616 Medline

21. R. Nasrallah, C. J. Imianowski, L. Bossini-Castillo, F. M. Grant, M. Dogan, L. Placek, L. Kozhaya, P. Kuo, F. Sadiyah, S. K. Whiteside, M. R. Mumbach, D. Glinos, P. Vardaka, C. E. Whyte, T. Lozano, T. Fujita, H. Fujii, A. Liston, S. Andrews, A. Cozzani, J. Yang, S. Mitra, E. Lugli, H. Y. Chang, D. Unutmaz, G. Trynka, R. Roychoudhuri, A distal

enhancer at risk locus 11q13.5 promotes suppression of colitis by T$_{reg}$ cells. *Nature* **583**, 447–452 (2020). doi:10.1038/s41586-020-2296-7 Medline

22. K. R. Sanson, R. E. Hanna, M. Hegde, K. F. Donovan, C. Strand, M. E. Sullender, E. W. Vaimberg, A. Goodale, D. E. Root, F. Piccioni, J. G. Doench, Optimized libraries for CRISPR-Cas9 genetic screens with multiple modalities. *Nat. Commun.* **9**, 5416 (2018). doi:10.1038/s41467-018-07901-8 Medline

23. S. Konermann, M. D. Brigham, A. E. Trevino, J. Joung, O. O. Abudayyeh, C. Barcena, P. D. Hsu, N. Habib, J. S. Gootenberg, H. Nishimasu, O. Nureki, F. Zhang, Genome-scale transcriptional activation by an engineered CRISPR-Cas9 complex. *Nature* **517**, 583–588 (2015). doi:10.1038/nature14136 Medline

24. S. M. Kaech, W. Cui, Transcriptional control of effector and memory CD8+ T cell differentiation. *Nat. Rev. Immunol.* **12**, 749–761 (2012). doi:10.1038/nri3307 Medline

25. J. Zhu, H. Yamane, W. E. Paul, Differentiation of effector CD4 T cell populations (*). *Annu. Rev. Immunol.* **28**, 445–489 (2010). doi:10.1146/annurev-immunol-030409-101212 Medline

26. V. Lazarevic, L. H. Glimcher, G. M. Lord, T-bet: A bridge between innate and adaptive immunity. *Nat. Rev. Immunol.* **13**, 777–789 (2013). doi:10.1038/nri3536 Medline

27. C. M. Evans, R. G. Jenner, Transcription factor interplay in T helper cell differentiation. *Brief. Funct. Genomics* **12**, 499–511 (2013). doi:10.1093/bfgp/elt025 Medline

28. A. H. Courtney, W.-L. Lo, A. Weiss, TCR signaling: Mechanisms of initiation and propagation. *Trends Biochem. Sci.* **43**, 108–123 (2018). doi:10.1016/j.tibs.2017.11.008 Medline

29. G. Gaud, R. Lesourne, P. E. Love, Regulatory mechanisms in T cell receptor signalling. *Nat. Rev. Immunol.* **18**, 485–497 (2018). doi:10.1038/s41577-018-0020-8 Medline

30. S. J. Holland, X. C. Liao, M. K. Mendenhall, X. Zhou, J. Pardo, P. Chu, C. Spencer, A. Fu, N. Sheng, P. Yu, E. Pali, A. Nagin, M. Shen, S. Yu, E. Chan, X. Wu, C. Li, M. Woisetschlager, G. Aversa, F. Kolbinger, M. K. Bennett, S. Molineaux, Y. Luo, D. G. Payan, H. S. Mancebo, J. Wu, Functional cloning of Src-like adapter protein-2 (SLAP-2), a novel inhibitor of antigen receptor signaling. *J. Exp. Med.* **194**, 1263–1276 (2001). doi:10.1084/jem.194.9.1263 Medline

31. J.-W. Shui, J. S. Boomer, J. Han, J. Xu, G. A. Dement, G. Zhou, T.-H. Tan, Hematopoietic progenitor kinase 1 negatively regulates T cell receptor signaling and T cell-mediated immune responses. *Nat. Immunol.* **8**, 84–91 (2007). doi:10.1038/ni1416 Medline

32. T. Hart, A. H. Y. Tong, K. Chan, J. Van Leeuwen, A. Seetharaman, M. Aregger, M. Chandrashekhar, N. Hustedt, S. Seth, A. Noonan, A. Habsid, O. Sizova, L. Nedyalkova, R. Climie, L. Tworzyanski, K. Lawson, M. A. Sartori, S. Alibeh, D. Tieu, S. Masud, P. Mero, A. Weiss, K. R. Brown, M. Usaj, M. Billmann, M. Rahman, M. Costanzo, C. L. Myers, B. J. Andrews, C. Boone, D. Durocher, J. Moffat, Evaluation and design of genome-wide CRISPR/SpCas9 knockout screens. *G3* **7**, 2719–2727 (2017). doi:10.1534/g3.117.041277 Medline

33. S. R. Ferdosi, R. Ewaisha, F. Moghadam, S. Krishna, J. G. Park, M. R. Ebrahimkhani, S. Kiani, K. S. Anderson, Multifunctional CRISPR-Cas9 with engineered immunosilenced

human T cell epitopes. *Nat. Commun.* **10**, 1842 (2019). doi:10.1038/s41467-019-09693-x Medline

34. H. Hu, H. Wang, Y. Xiao, J. Jin, J.-H. Chang, Q. Zou, X. Xie, X. Cheng, S.-C. Sun, Otud7b facilitates T cell activation and inflammatory responses by regulating Zap70 ubiquitination. *J. Exp. Med.* **213**, 399–414 (2016). doi:10.1084/jem.20151426 Medline

35. E. P. Mimitou, A. Cheng, A. Montalbano, S. Hao, M. Stoeckius, M. Legut, T. Roush, A. Herrera, E. Papalexi, Z. Ouyang, R. Satija, N. E. Sanjana, S. B. Koralov, P. Smibert, Multiplexed detection of proteins, transcriptomes, clonotypes and CRISPR perturbations in single cells. *Nat. Methods* **16**, 409–412 (2019). doi:10.1038/s41592-019-0392-0 Medline

36. C. Alda-Catalinas, D. Bredikhin, I. Hernando-Herraez, F. Santos, O. Kubinyecz, M. A. Eckersley-Maslin, O. Stegle, W. Reik, A single-cell transcriptomics CRISPR-activation screen identifies epigenetic regulators of the zygotic genome activation program. *Cell Syst.* **11**, 25–41.e9 (2020). doi:10.1016/j.cels.2020.06.004 Medline

37. J. M. Replogle, T. M. Norman, A. Xu, J. A. Hussmann, J. Chen, J. Z. Cogan, E. J. Meer, J. M. Terry, D. P. Riordan, N. Srinivas, I. T. Fiddes, J. G. Arthur, L. J. Alvarado, K. A. Pfeiffer, T. S. Mikkelsen, J. S. Weissman, B. Adamson, Combinatorial single-cell CRISPR screens by direct guide RNA capture and targeted sequencing. *Nat. Biotechnol.* **38**, 954–961 (2020). doi:10.1038/s41587-020-0470-y Medline

38. P. I. Thakore, A. M. D'Ippolito, L. Song, A. Safi, N. K. Shivakumar, A. M. Kabadi, T. E. Reddy, G. E. Crawford, C. A. Gersbach, Highly specific epigenome editing by CRISPR-Cas9 repressors for silencing of distal regulatory elements. *Nat. Methods* **12**, 1143–1149 (2015). doi:10.1038/nmeth.3630 Medline

39. C. P. Fulco, M. Munschauer, R. Anyoha, G. Munson, S. R. Grossman, E. M. Perez, M. Kane, B. Cleary, E. S. Lander, J. M. Engreitz, Systematic mapping of functional enhancer-promoter connections with CRISPR interference. *Science* **354**, 769–773 (2016). doi:10.1126/science.aag2445 Medline

40. X. Xu, L. S. Qi, A CRISPR-dCas toolbox for genetic engineering and synthetic biology. *J. Mol. Biol.* **431**, 34–47 (2019). doi:10.1016/j.jmb.2018.06.037 Medline

41. I. Chun, K. H. Kim, Y.-H. Chiang, W. Xie, Y. G. G. Lee, R. Pajarillo, A. Rotolo, O. Shestova, S. J. Hong, M. Abdel-Mohsen, M. Wysocka, H. J. Ballard, D. M. Barrett, A. D. Posey, D. Powell Jr., S. I. Gill, S. J. Schuster, S. K. Barta, A. H. Rook, C. H. June, M. Ruella, CRISPR-Cas9 knock out of CD5 enhances the anti-tumor activity of chimeric Antigen Receptor T cells. *Blood* **136** (Supplement 1), 51–52 (2020). doi:10.1182/blood-2020-136860

42. R. C. Lynn, E. W. Weber, E. Sotillo, D. Gennert, P. Xu, Z. Good, H. Anbunathan, J. Lattin, R. Jones, V. Tieu, S. Nagaraja, J. Granja, C. F. A. de Bourcy, R. Majzner, A. T. Satpathy, S. R. Quake, M. Monje, H. Y. Chang, C. L. Mackall, c-Jun overexpression in CAR T cells induces exhaustion resistance. *Nature* **576**, 293–300 (2019). doi:10.1038/s41586-019-1805-z Medline

43. P. Datlinger, A. F. Rendeiro, C. Schmidl, T. Krausgruber, P. Traxler, J. Klughammer, L. C. Schuster, A. Kuchler, D. Alpar, C. Bock, Pooled CRISPR screening with single-cell

transcriptome readout. *Nat. Methods* **14**, 297–301 (2017). doi:10.1038/nmeth.4177 Medline

44. J. W. Freimer, O. Shaked, S. Naqvi, N. Sinnott-Armstrong, A. Kathiria, A. F. Chen, J. T. Cortez, W. J. Greenleaf, J. K. Pritchard, A. Marson, Systematic discovery and perturbation of regulatory genes in human T cells reveals the architecture of immune networks. bioRxiv 2021.04.18.440363 (2021); https://www.biorxiv.org/content/10.1101/2021.04.18.440363v1.

45. W. Li, H. Xu, T. Xiao, L. Cong, M. I. Love, F. Zhang, R. A. Irizarry, J. S. Liu, M. Brown, X. S. Liu, MAGeCK enables robust identification of essential genes from genome-scale CRISPR/Cas9 knockout screens. *Genome Biol.* **15**, 554 (2014). doi:10.1186/s13059-014-0554-4 Medline

46. G. Korotkevich, V. Sukhov, N. Budin, B. Shpak, M. N. Artyomov, A. Sergushichev, Fast gene set enrichment analysis. bioRxiv 060012 (2016); https://www.biorxiv.org/content/10.1101/060012v3.

47. H. K. Finucane, B. Bulik-Sullivan, A. Gusev, G. Trynka, Y. Reshef, P.-R. Loh, V. Anttila, H. Xu, C. Zang, K. Farh, S. Ripke, F. R. Day, S. Purcell, E. Stahl, S. Lindstrom, J. R. B. Perry, Y. Okada, S. Raychaudhuri, M. J. Daly, N. Patterson, B. M. Neale, A. L. Price; ReproGen Consortium; Schizophrenia Working Group of the Psychiatric Genomics Consortium; RACI Consortium, Partitioning heritability by functional annotation using genome-wide association summary statistics. *Nat. Genet.* **47**, 1228–1235 (2015). doi:10.1038/ng.3404 Medline

48. M. A. Horlbeck, L. A. Gilbert, J. E. Villalta, B. Adamson, R. A. Pak, Y. Chen, A. P. Fields, C. Y. Park, J. E. Corn, M. Kampmann, J. S. Weissman, Compact and highly active next-generation libraries for CRISPR-mediated gene repression and activation. *eLife* **5**, e19760 (2016). doi:10.7554/eLife.19760 Medline

49. M. Martin, Cutadapt removes adapter sequences from high-throughput sequencing reads. *EMBnet. J.* **17**, 10–12 (2011). doi:10.14806/ej.17.1.200

50. A. Dobin, C. A. Davis, F. Schlesinger, J. Drenkow, C. Zaleski, S. Jha, P. Batut, M. Chaisson, T. R. Gingeras, STAR: Ultrafast universal RNA-seq aligner. *Bioinformatics* **29**, 15–21 (2013). doi:10.1093/bioinformatics/bts635 Medline

51. Y. Liao, G. K. Smyth, W. Shi, featureCounts: An efficient general purpose program for assigning sequence reads to genomic features. *Bioinformatics* **30**, 923–930 (2014). doi:10.1093/bioinformatics/btt656 Medline

52. M. E. Ritchie, B. Phipson, D. Wu, Y. Hu, C. W. Law, W. Shi, G. K. Smyth, limma powers differential expression analyses for RNA-sequencing and microarray studies. *Nucleic Acids Res.* **43**, e47 (2015). doi:10.1093/nar/gkv007 Medline

53. H. Heaton, A. M. Talman, A. Knights, M. Imaz, D. J. Gaffney, R. Durbin, M. Hemberg, M. K. N. Lawniczak, Souporcell: Robust clustering of single-cell RNA-seq data by genotype without reference genotypes. *Nat. Methods* **17**, 615–620 (2020). doi:10.1038/s41592-020-0820-1 Medline

54. R. Satija, J. A. Farrell, D. Gennert, A. F. Schier, A. Regev, Spatial reconstruction of single-cell gene expression data. *Nat. Biotechnol.* **33**, 495–502 (2015). doi:10.1038/nbt.3192 Medline

55. C. Hafemeister, R. Satija, Normalization and variance stabilization of single-cell RNA-seq data using regularized negative binomial regression. *Genome Biol.* **20**, 296 (2019). doi:10.1186/s13059-019-1874-1 Medline

56. Z. Steinhart, Code repository for: "CRISPR activation and interference screens decode stimulation responses in primary human T cells," Zenodo (2022); https://doi.org/10.5281/zenodo.578465.

57. B. J. Schmiedel, D. Singh, A. Madrigal, A. G. Valdovino-Gonzalez, B. M. White, J. Zapardiel-Gonzalo, B. Ha, G. Altay, J. A. Greenbaum, G. McVicker, G. Seumois, A. Rao, M. Kronenberg, B. Peters, P. Vijayanand, Impact of genetic polymorphisms on human immune cell gene expression. *Cell* **175**, 1701–1715.e16 (2018). doi:10.1016/j.cell.2018.10.022 Medline

58. S. V. Aguilar, O. Aguilar, R. Allan, E. A. D. Amir, V. Angeli, M. N. Artyomov, N. Asinovski, J. Astarita, K. F. Austen, G. Bajpai, N. Barrett, A. Baysoy, C. Benoist, A. Bellemare-Pelletier, B. Berg, A. Best, N. Bezman, D. Blair, J. M. Blander, M. Bogunovic, P. Brennan, M. Brenner, B. Brown, M. Buechler, J. Buenrostro, M. A. Casanova, K. Choi, A. Chow, A. Chudnovskiy, D. Cipoletta, N. Cohen, J. J. Collins, M. Colonna, A. Cook, J. Costello, V. Cremasco, T. Crowl, K. Crozat, R. Cruse, J. D'Angelo, M. Dalod, S. Davis, C. Demiralp, T. Deng, J. V. Desai, F. Desland, M. Dhainaut, J. Ding, A. Doedens, C. Dominguez, G. Doran, R. Dress, M. Dustin, D. Dwyer, I. Dzhagalov, K. Elpek, A. Ergun, J. Ericson, E. Esomonu, K. Fairfax, A. Fletcher, M. Frascoli, A. Fuchs, A. Gainullina, S. Gal-Oz, M. Gallagher, E. Gautier, R. Gazit, S. Gibbings, M. Giraud, F. Ginhoux, A. Goldrath, D. Gotthardt, D. Gray, M. Greter, R. Grieshaber-Bouyer, M. Guilliams, S. Haidermota, R. Hardy, D. Hashimoto, J. Helft, D. Hendricks, T. Heng, J. Hill, G. Hyatt, J. Idoyaga, C. Jakubzick, J. Jarjoura, D. Jepson, B. Jia, R. Jianu, T. Johanson, S. Jordan, V. Jojic, S. Jordan, Y. Kamimura, V. Kana, J. Kang, V. Kapoor, E. Kenigsberg, A. Kent, C. Kim, E. Kim, F. Kim, J. Kim, K. Kim, E. Kiner, J. Knell, D. Koller, L. Kozinn, K. Krchma, T. Kreslavsky, M. Kronenberg, W.-H. Kwan, D. Laidlaw, V. Lam, L. Lanier, C. Laplace, C. Lareau, Y. Lavin, K. J. Lavine, A. Leader, M. Leboeuf, J. Lee, J. Lee, B. Li, H. Li, Y. Li, M. S. Lionakis, H. Luche, L. Lynch, A. Magen, B. Maier, D. Malhotra, N. Malhotra, M. Malissen, A. Maslova, D. Mathis, A. McFarland, M. Merad, E. Meunier, J. Miller, J. Milner, M. Mingueneau, G. Min-Oo, P. Monach, D. Moodley, A. Mortha, M. Morvan, S. Mostafavi, S. Muller, C. Muus, T. Nabekura, T. N. Rao, V. Narang, K. Narayan, H. Ner-Gaon, Q. Nguyen, P. A. Nigrovic, G. Novakovsky, S. Nutt, K. Omilusik, A. Ortiz-Lopez, H. Paidassi, H. Paik, M. Painter, M. Paynich, V. Peng, M. Potempa, R. Pradhan, J. Price, Y. Qi, Y. Qi, S. Quon, R. Ramirez, D. Ramanan, G. Randolph, A. Regev, A. Rhoads, M. Robinette, S. Rose, D. Rossi, K. Rothamel, R. Sachidanandam, P. Sathe, C. Scott, K. Seddu, P. See, A. Sergushichev, L. Shaw, T. Shay, A. Shemesh, S. Shinton, J. Shyer, M. Sieweke, C. Smillie, L. Spel, N. Spidale, G. Stifano, A. Subramanian, J. Sun, K. Sylvia, J. Tellier, S. This, E. Tomasello, H. Todorov, S. Turley, B. Vijaykumar, A. Wagers, E. Wakamatsu, C. Wang, P. L. Wang, A. Wroblewska, J. Wu, E. Yang, L. Yang, A. Yim, L. S. Yng, H. Yoshida, B. Yu, Y. Zhou, Y. Zhu, C. Ziemkiewicz; Immunological Genome Project, ImmGen at 15. *Nat. Immunol.* **21**, 700–703 (2020). doi:10.1038/s41590-020-0687-4 Medline

59. B. P. Nicolet, A. Guislain, F. P. J. van Alphen, R. Gomez-Eerland, T. N. M. Schumacher, M. van den Biggelaar, M. C. Wolkers, CD29 identifies IFN-γ-producing human CD8^{+} T

cells with an increased cytotoxic potential. *Proc. Natl. Acad. Sci. U.S.A.* **117**, 6686–6696 (2020). doi:10.1073/pnas.1913940117 Medline